Materials Advances

REVIEW

View Article Online
View Journal | View Issue

Cite this: *Mater. Adv.*, 2025, 6, 4623

Clay-based photocatalytic membranes: low-cost alternative materials for water treatment

Chidinma G. Olorunnisola, *[ab] Damilare Olorunnisola,[abc] Morenike. O. Adesina,[abc] Moses O. Alfred,[ac] Abisola O. Egbedina,[d] Oluwayimika O. Oluokun,[e] Martins O. Omorogie,[ac] Emmanuel I. Unuabonah[ac] and Andreas Taubert *[b]

Received 3rd April 2025,
Accepted 17th May 2025

DOI: 10.1039/d5ma00313j

rsc.li/materials-advances

The integration of photocatalysis and membrane filtration has emerged as a promising technology for water treatment, offering the dual advantages of physical separation and degradation of organic pollutants. However, the high cost and complexity of current membrane materials limit their large-scale application. This review aims to provide a comprehensive overview of clay-based photocatalytic membranes as a low-cost, sustainable alternative for water purification. It highlights the natural abundance, structural versatility, and surface functionality of clay minerals that make them ideal candidates for membrane fabrication. The review discusses various fabrication techniques and key factors affecting membrane structure and performance. Furthermore, it includes current applications of these membranes in pollutant degradation, alongside an evaluation of challenges and future perspectives for practical deployment in water treatment systems.

1. Introduction

Population growth and urbanization have increased the number of users and the uses of water, making water resources scarcer and more polluted. Globally, water scarcity and water pollution are threatening human, economic, and environmental health.[1] The sixth goal of the seventeen United Nation's sustainable development goals is to "ensure availability and sustainable management of water and sanitation for all". The achievement of this goal would benefit mankind immensely given the significance of clean water for overall socioeconomic development and quality of life, including human and environmental health. Although conventional water purification techniques such as ozonation, adsorption, UV-radiation, chlorination, bio-oxidation, coagulation, *etc.*, have been successful in addressing water pollution issues, they generally fail in the efficient removal of recalcitrant chemical compounds from water. In addition, most of these techniques generate toxic intermediates and in some other cases, they are less efficient for the treatment of large volumes of water with trace concentrations of pollutants.[2] However, membrane filtration has recently emerged as a successful alternative to overcome these limitations.

In recent years, membrane filtration has increasingly been utilized in wastewater treatment and has provided an affordable alternative for sustainable water reclamation. Unfortunately, this goes along with membrane fouling, which leads to a decline in performance as a result of a sharp rise of the transmembrane pressure, flux decline, and even system failure.[3,4] Additionally, the removal of contaminants with molecular sizes smaller than the membrane pores and the existence of emerging low molecular weight contaminants occurring at trace concentrations are even more challenging for the traditional membrane filtration.[5]

Membrane anti-fouling techniques such as physical, hydraulic, or chemical cleaning of the membrane have been applied to manage the problem;[6] yet, these anti-fouling techniques do impair the efficiency of the membrane. This obviously increases the overall running costs of the process. In addition, the need to purchase, transport and store chemicals used for chemical cleaning of the membrane and their eventual safe disposal is not only laborious but also results in increased cost for the entire water treatment process. Overall, all these aspects make membrane filtration an unfeasible option for rural communities in developing countries, as they lack the required resources to effectively use the membrane technology for water treatment.

Photocatalysis on the other hand is generally eco-friendly. It uses *in situ* generated radicals for non-selective degradation of

[a] *African Centre of Excellence for Water and Environment Research (ACEWATER), Redeemer's University, PMB 230, Ede, Osun State, Nigeria. E-mail: ugwujac@run.edu.ng*
[b] *Institute of Chemistry, University of Potsdam, D-14476 Potsdam, Germany. E-mail: ataubert@uni-potsdam.de*
[c] *Department of Chemical Sciences, Redeemer's University, PMB 230, Ede, Osun State, Nigeria*
[d] *Department of Chemistry, University of Ibadan, Nigeria*
[e] *Department of Metallurgical Engineering, Vaal University of Technology, South Africa*

(organic and biological) contaminants until total mineralization to carbon dioxide, water and inorganic ions or until non-toxic biodegradable small molecules are formed.[7] As a result, the combination of photocatalysis and membrane processes has attracted increasing attention for water and wastewater treatment, since it incorporates the advantages of membrane separation and photocatalytic degradation of pollutants.[8] Therefore, immobilizing semiconductor photocatalysts on membrane surfaces improves the filtration performance of membranes through photodegradation of pollutants to non-harmful products and serves as an *in situ* method of fouling management *via* photocatalysis of fouling agents directly on the membrane surface.[9] This gives the technology a double-edged positive effect, and the challenge of disposing secondary waste from maintenance and cleaning operations of the membrane is significantly reduced. More so, the photocatalytic membrane technique utilized for water purification minimizes environmental hazards from the process through mineralization of organic contaminants to CO_2 and H_2O, and optimizes the economic aspects of the process *via* an active and inherent anti-fouling and self-cleaning ability of the membranes. This makes it highly attractive for industrial and continuous flow applications.[10]

There are basically two types of membranes: polymeric and ceramic. Polymeric membranes have been widely utilised and studied for water treatment. Polyvinylidene fluoride (PVDF), polyacrylonitrile (PAN), and polytetrafluoroethylene (PTFE) and other polymer membranes have gained widespread application due to their flexibility, cost-effectiveness, and ease of fabrication.[11] Recent studies highlight their enhanced resistance to UV radiation, particularly in hydrophobic configurations, enabling prolonged service life in specific environments.[5] However, their performance under extreme chemical or photochemical conditions, such as high concentrations of hydroxyl radicals and prolonged ultraviolet (UV) exposure, remains a challenge for broader application in photocatalytic water treatment systems.[12]

On the other hand, ceramic membranes offer better thermal, chemical and mechanical stability; they are also more resistant to the physical damage during use and under photocatalytic conditions.[13] Additionally, the existence of abundant hydrophilic hydroxyl groups on the surface of ceramic membranes somewhat mitigates membrane fouling. All these properties currently endear ceramic materials to materials scientists as a desirable substrate for the fabrication of photocatalytic membranes for water treatment.[14–17]

Nevertheless, the high cost of the raw materials and the high amount of energy required for the production of ceramic membranes are crucial disadvantages.[18] However, the use of clay minerals, which have outstanding properties such as high stability, natural abundance, environmental friendliness, low-cost, and regularly arranged silica-alumina framework, does serve to mitigate these challenges in the fabrication of photocatalytic membranes.[6] Firstly, most clay minerals are highly hydrophilic, which makes them desirable for membrane development and particularly advantageous for water filtration.[13,19] Secondly, clay minerals have abundant adsorption and reactive sites leading to high adsorption capacities and catalytic performance, strong cation exchangeability for accelerating catalytic reactions, and a suitable surface electronegativity for improving charge carrier separation.[20,21] Finally, clay minerals have also been shown to enhance the photocatalytic performance of bare semiconductor photocatalysts.[22,23] For example, ZnO, TiO_2 and graphitic carbon nitride (g-C_3N_4) have been assembled into layered silicate clay mineral to construct 0D/2D or 2D/2D hybrid structures, which effectively mitigate the problem of poor light absorption.[22,23] Thus, clay minerals can find further application as support in the development of catalytic membranes.

Several review articles have been published on ceramic membranes[24–26] and clay composite photocatalysts for the degradation of pollutants in water. For example, a recent article reviewed and discussed the photocatalytic advantages of doping three different types of clay minerals, namely, kaolinite, montmorillonite and rectorite, with semiconductors.[6] In another article, the utilization of clay composite photocatalysts for the removal of emerging micropollutants and for microbial inactivation in water was discussed.[27] Furthermore, a critical review on the recent progress of ceramic membranes for water treatment has been published as well.[26]

However, to the best of our knowledge, the utilization of clay for the development of photocatalytic membranes has not been critically reviewed as only a few reports are available with respect to the use of clay-based photocatalytic membranes. This is intriguing because the use of clay (a rather abundant resource) for the fabrication of photocatalytic membranes would provide a quite effective solution to the challenges encountered with large scale application of inorganic membranes, including the high production cost of conventional ceramic materials that utilize alumina, zirconia or silica.[5,25]

This review, therefore, focuses on semiconductor-doped clay-based membranes, providing an overview of their fabrication and application in water treatment for the removal of dyes, pharmaceutical residues and heavy metals. This article serves as a resource for researchers interested in developing or improving clay-based photocatalytic membranes for water treatment.

2. Fabrication of clay-based membranes

Clay-based membranes can be prepared *via* different methods such as tape casting, slip casting, extrusion, and others. Furthermore, clay-based membranes can be obtained in different configurations including flat sheet, tubular, and multichannel models, depending on the shaping method used. Irrespective of the fabrication technique of clay-based membranes, the nature of the precursor material(s) and additives, pore size, porosity, grain growth and formation of micro-cracks are important factors that directly affect the properties of the final membranes. As a result, there is a large variability in membrane fabrication processes; these processes will be discussed next. Table 1 contains the comparative overview of these fabrication methods.

Table 1 Comparative overview of fabrication methods of clay-based membranes

Fabrication method	Principle	Porosity and thickness	Advantages	Limitations
Tape casting	A clay slurry is spread into a thin tape using a disc or doctor blade, dried, and then sintered	Produces flat membranes of uniform thickness and moderate porosity	Enables uniform thickness; good control over layer composition	Limited to flat geometries and drying cracks can occur without careful control
Slip casting	A clay slurry is poured into a mold; water absorption leads to solid layer formation	Produces thick and dense membranes; porosity depends on particle size and drying rate	Simple and inexpensive; suitable for thick supports	Long drying time; difficulty in achieving thin layers or high porosity
Extrusion	Clay is forced through a shaped die under pressure to form hollow or tubular structures	Can produce dense or porous tubular membranes depending on clay and additives	Good for continuous production; suitable for tubular geometries	Requires specialized equipment; porosity tuning is more difficult
Pressing	Dry or semi-dry clay powder (often mixed with binders) is loaded into a die and compacted under high uniaxial or isostatic pressure, then sintered to form a dense membrane support	Can yield large-area or tubular membranes with porosity 20–50% and uniform wall thickness (0.5–2 mm)	Continuous production; ideal for hollow fibers and tubes; high surface–volume ratio	Limited to simple shapes (discs, plates); low inherent porosity unless pore formers are used
Phase inversion	Clay is forced through a shaped die under pressure to form hollow or tubular structures	Can produce dense or porous tubular membranes depending on clay and additives	Good for continuous production; suitable for tubular geometries	Could lead to poor mechanical strength and uneven distribution of clay particles

2.1. Tape casting

Tape casting is a thermal forming process that involves three main steps: (i) the preparation of the clay slurry with the desired viscosity, (ii) the casting step, which is carried out using a disc or doctor blade, and (iii) sintering. In the preparation of clay slurry, it is important to note that the viscosity of the slurry should be in the range of 100–130 Poise (10^{-1} Ns m^{-2}).[28] The doctor blade, set to a suitable thickness (Fig. 1), is used to spread the clay slurry evenly, ensuring a uniform thickness. The slurry is then cut into the necessary forms (circular, rectangular, or square).

For instance, tape casting was used for the fabrication of a kaolinite circular microfiltration membrane.[30] The kaolinite slurry was prepared without any additives or binders. The membrane had an average pore size, porosity, and water permeability of 5.88 μm, 24.30% and 0.9865 L m^{-2} h^{-1} k^{-1} Pa^{-1}, respectively.[30]

To improve the porosity and overall properties of clay-based membranes, the addition of inorganic additives into the slurry before casting has been explored. For instance, a microfiltration membrane consisting of 47.4% of clay, 22.9% of kaolinite, 21% of water, 3.9% of sodium carbonate, 2.4% of sodium metasilicate and boric acid was fabricated *via* tape casting.[31] The paste was then cast over gypsum in the shape of circular compact disks using a stainless-steel ring and was subsequently sintered. The porosity and the average pore diameter of the resulting membrane were 43.6% and 0.58 μm, respectively.

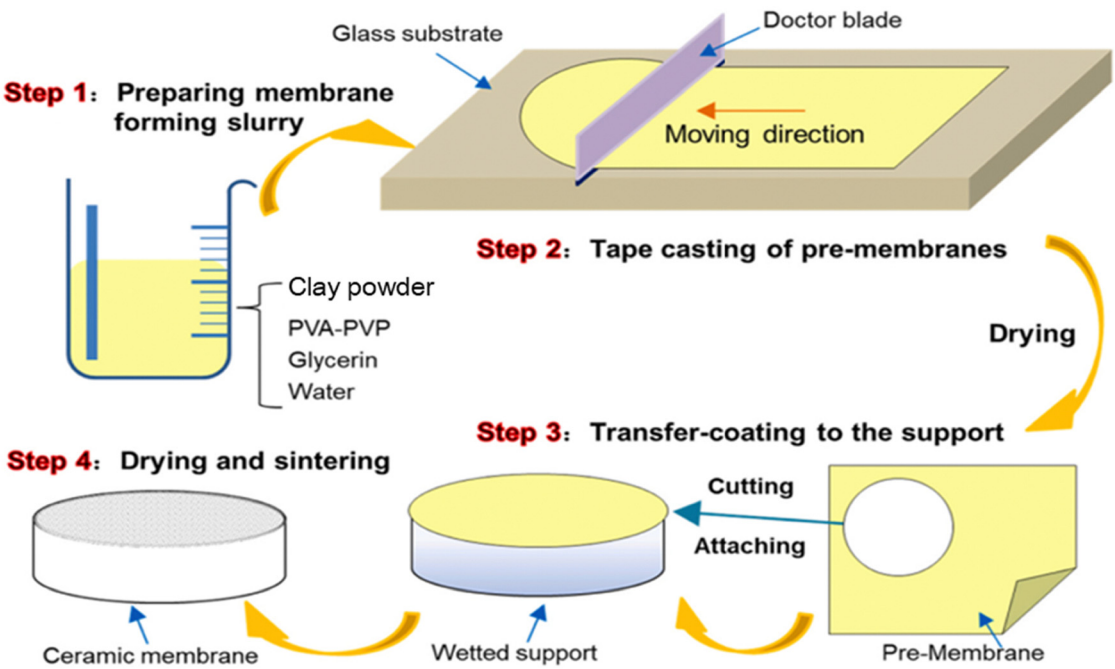

Fig. 1 Schematic diagram of the tape casting process. Figure reprinted from ref. 29 with permission from Elsevier, Copyright 2025.

These values are better than the results obtained by Ahmed *et al.*[30]

Microfiltration membranes were also prepared using different compositions of kaolin (37.03 wt%), quartz (11.11 wt%), feldspar (7.40 wt%), activated carbon (7.4 wt%), boric acid (3.7 wt%), sodium metasilicate (3.7 wt%), titanium dioxide (3.7 wt%) and water (25.92 wt%) *via* paste casting. The final membrane had an average pore diameter and porosity of 2.56 μm and 18.88%, respectively.[32] However, mixing the slurry of kaolin and other additives with activated carbon enhanced the porosity of the membrane during the sintering process.[32]

Despite the advantages of tape or paste casting in preparing clay-based membranes of different pore sizes and porosity, it is not without some drawbacks. For instance, this technique results in poor precision with respect to the shape of the membrane arising from corrosion or shrinking of the plaster mold. Furthermore, paste casting is time consuming when applied to a slurry made from fine powder. An attempt to overcome this problem by the pressing method invariably increased the overall process/production cost.[28]

2.2. Slip casting

The slip casting method is used in the preparation of clay-based membranes due to its ease of operation and lower cost when compared with other techniques.[28] The primary distinction between slip casting and tape casting is that the former is utilized to create thin sheet membranes, whereas the latter is employed to create membranes with more intricate shapes. During slip casting, a microporous plaster of Paris mold is filled with a slurry or slip that contains the materials needed to fabricate the membrane. A capillary suction pressure can draw fluid from the slurry into the mold owing to the porous nature of the mold, leaving an inner layer of solid behind. The cast is allowed to dry after the appropriate cast thickness is reached. The final result is created by heating and sintering the cast once it has dried.[33]

Clay-based membranes were first fabricated *via* slip casting combined with electrophoresis by Mohammadi and Pak.[34] The work was focused on enhancing the performance of zeolite membranes by using a kaolin support containing 58.62 wt% of SiO_2 and 28.8 wt% of Al_2O_3. The viscosity of the slurry was maintained by the addition of *ca.* 1.3 g of sodium triphosphate, which produced the desired slurry density of 1.5 g cm^{-3}. This is crucial for preventing the slurry from sticking to the mold. Electrophoresis was carried out at 10 V and 0.25 A since the kaolin surface was negatively charged. Hence, the slurry was deposited on the anode to form a tubular membrane which was sintered between 800 and 1200 °C for 180 min. The membrane porosity increased with sintering temperature, yielding a membrane with large pores.

However, slip casting has the disadvantage of long casting time because it involves a slow drying process. This has limited its use in recent years for the fabrication of clay-based membranes. In addition, it is difficult to control the membrane wall thickness during the drying stage, because it is dependent on the slurry condition and casting time.[33]

2.3. Extrusion

Extrusion is mostly used in the fabrication of tubular ceramic membranes. In this process, a clay/additive mixture is compacted and formed by pushing it through a nozzle in a screw (Auger) extruder or piston (ram) extruder.[33] In this process, it is important that the moisture content of the slurry is higher than 15% because this can affect the viscosity of the fluid mass and the functional properties of the extrudates and their storage conditions.[28]

In short, there are five basic steps involved in the extrusion: (i) blending – this ensures that the ceramic compositions are uniformly mixed and distributed in a liquid medium, (ii) pugging – the mix is placed in a pug mill to remove air and form a uniform liquid layer around all particles, (iii) extrusion – the de-aired mix is ejected through a die by the application of pressure or screw movement, (iv) cutting and drying – after the desired length of the material mix is extruded, it is cut and dried, and (v) sintering – the dried material is sintered at the desired temperature to obtain the final ceramic (membrane).[35]

For example, a monolayered ultrafiltration clay-based membrane, consisting of a single uniform layer, was fabricated using extrusion.[36] To start, a homogeneous paste was prepared using 400 g of a mixture of clay, organic additives (amijel, *i.e.*, pre-gelated starch as a plasticizer; methocel, *i.e.*, methylcellulose as a binder; starch as a porogen) and distilled water. This paste was aged for a day and then extruded into tubes of 6 mm internal diameter which were sintered at different temperatures for 3 h to obtain the ceramic membranes. Scanning electron microscopy (SEM) shows that there is a significant change in the density of the sintered material at 950 °C, 1000 °C, and 1050 °C. The membrane sintered at 1000 °C shows a homogeneous structure. It has a membrane permeability of 21.2 L h^{-1} m^{-2} bar^{-1}, making it suitable for ultrafiltration. At 1050 °C, the glassy phase was reached.

Extrusion favors the production of tubular ceramic membranes from clay. The resulting membranes have a higher surface area per volume ratio when compared to flat, disc or planar membranes. This is evident in a number of studies that have employed extrusion for the preparation of tubular clay membranes.[28] The data indicate that simple mixing of clay with distilled water is sufficient for slurry preparation, while amijel and methocel may be added to the slurry to improve the rheological properties of the slurry. Moreover, the sintering temperature of the clay slurry is always in the range of 800 to 1250 °C except when alumina is added into the slurry. In that case, the sintering temperature could be as high as 1600 °C.[28] However, despite the wide adoption of the extrusion technique in the development of clay-based membranes, it requires a complex preparation process, high pressure to move the mixture, and is overall quite time consuming.[37]

2.4. Pressing

Pressing is the simplest fabrication process for ceramic membranes as no slurry preparation is required. Selected precursors are loaded into steel or tungsten carbide forms and compacted

at pressures necessary for compaction. Uniaxial die pressing and isostatic pressing are widely used for dry powder compaction (powders with <2 wt% water) and for semidry powder compaction (powders with *ca.* 5–20 wt% water).[33] Pressing produces clay-based membranes with high mechanical strength that are viable for high-pressure applications.

Vasanth *et al.* reported the fabrication of macroporous clay-based membranes *via* uniaxial dry pressing. The membrane was prepared by combining 4 mL of 2 wt% aqueous polyvinyl alcohol with kaolin (40%), quartz (15%), calcium carbonate (25%), sodium carbonate (10%), boric acid (5%) and sodium metasilicate (5%). The mixture was compacted at 50 MPa, dried and sintered at different temperatures between 900 and 1000 °C for 6 h. The optimum membrane with 30% porosity, 28 MPa mechanical strength and an average pore size of 3.45 μm was obtained at a sintering temperature of 950 °C.[38] Similarly, a clay-based ceramic membrane support was fabricated from a slurry consisting of 14.45 g of kaolin, 14.73 g of pyrophyllite, 5.60 g of feldspar, 17.58 g of ball clay, 26.59 g of quartz, 17.14 g of calcium carbonate and 4 mL of 2 wt% polyvinyl alcohol solution.[39] The mixture was also pressed at 50 MPa and was sintered at 950 °C for 6 h.

The pressing method typically produces symmetrical membranes, meaning they have a uniform structure and pore distribution throughout, rather than an asymmetrical design with a graded pore structure. Additionally, this method often requires high-pressure equipment and precise control, leading to increased operational costs.[37]

2.5. Phase inversion

Phase inversion was invented by Loeb and Sourirajan in the early 1960s for the fabrication of polymeric membranes.[40] It has subsequently been adapted for the production of ceramic membranes by using mixtures of suitable ceramic powders as the main component with polymeric binders, which are burnt away during sintering.[41] Generally, in the phase inversion process, ceramic powders with a suitable solvent are milled for a day and then mixed for one more day after the addition of a suitable polymeric binder. Thereafter, the suspension is extruded through a double cylinder nozzle placed close to a non-solvent bath and then submerged in the non-solvent bath.[26] This immersion induces phase separation, where the solvent diffuses out while the non-solvent penetrates, forming a porous structure. The resulting membrane is dried and sintered to achieve the desired mechanical strength and filtration properties. More recently, spinnerets with double and triple orifices have been used to fabricate single and double layer ceramic hollow fibre membranes, respectively.[42,43]

In phase inversion processes, typically two types of pores (finger-like and sponge-like voids) form in the final membranes. The finger-like shape of the pores is caused by agglomeration of the inorganic ceramic particles and lack of de-airing during the phase inversion. Although these pores may be preferable over the sponge-like pores due to less resistance to fluid movement, the finger-like pores significantly reduce the mechanical strength of the membrane and hence pose challenges for the overall stability of the membrane.[26,41]

Phase inversion coupled with extrusion and sintering has been employed for making mullite-type hollow fiber clay membranes from ball clay.[44] The clay suspensions were prepared by mixing different compositions of ball clay, polyethylene glycol (PEG 30), poly(ethersulfone), and *N*-methyl-2-pyrrolidone; these mixtures were then milled for 48 h. The suspensions were degassed for 1 h and then extruded through a tube-in-orifice spinneret. The resultant hollow fibre was immersed in tap water overnight to ensure complete solvent/non-solvent exchange. Thereafter, the extruded tube was sintered at different temperatures between 1150 and 1300 °C. The optimum sintering temperature (1250 °C) produced a membrane with 55.8 MPa mechanical strength, 50.5% porosity, 0.61 μm pore size and 1286 L h^{-1} m^{-2} bar^{-1} flux.

In another study, the effect of the coagulation bath (demineralized water or aqueous salt solutions) on the performance of polyvinyl chloride (PVC)/bentonite flat sheet ultrafiltration membranes prepared using phase inversion from *N*,*N*-dimethylacetamide was investigated.[45] The presence of salts (NH_4Cl, NaCl, KCl, $MgCl_2$ and $CaCl_2$) reduced the phase separation (*i.e.*, the tendency of the solution to separate into two phases) of the PVC casting solution owing to reduction in the thermodynamic stability of the system. However, KCl exhibited the minimum flocculation value (0.59), while NH_4Cl had the maximum flocculation value (1.59) and the least effect on the flocculation of PVC. Hence, among the salts used, the KCl coagulation bath provided the best performing clay-based membrane with 5% bentonite loading. The enhanced membrane performance from using KCl over demineralized water coagulation bath is primarily attributed to improved surface pore density with finger-like structures, higher surface and bulk porosity, and antifouling behavior.

Despite the efficiency of clay-based ceramic membranes prepared from phase inversion, they suffer from poor mechanical strength. This is due to the highly porous structure and large surface area obtained through the fabrication process.[26] Hence, more recent research has focused on the fabrication of low-cost clay-based membranes in hollow fibre configuration.[26]

3. Fabrication of clay-based photocatalytic membranes

Clay minerals are not only viable as low-cost membrane substrates, but also play an active role in enhancing photocatalytic performance. Their abundant surface functional groups and strong cation exchange capacity facilitate adsorption and catalytic reactions. Additionally, clays possess stable frameworks that support catalyst recycling, surface electronegativity that promotes effective electron–hole separation, and unique layered or tubular structures that enable the assembly of multidimensional heterojunctions with photocatalysts such as TiO_2, ZnO and WO_3.[46,47] These features make clays both structurally and functionally beneficial for the development of

photocatalytic membranes. For example, Bi_2O_3 incorporated into montmorillonite (MMT) clay *via* intercalation exhibits an increased efficiency for the photocatalytic degradation of Congo red under visible-light irradiation when compared with unsupported Bi_2O_3.[48] This improved performance is attributed to increased catalytic active sites provided by the clay. Similarly, halloysite clay, due to its tubular morphology and surface charge, has also improved the photocatalytic degradation of methyl orange when used to support $W_{18}O_{49}$ nanocrystals (halloysite@$W_{18}O_{49}$).[49] These examples confirm that clays enhance light-driven photocatalysis by increasing the surface area, stabilizing the photocatalysts, and facilitating better pollutant–photocatalyst interactions under both UV and visible-light irradiation.

The integration of photocatalytic particles on the surface of prepared membranes or in the interlayer of membranes can be done *via* two major techniques: (i) *in situ* incorporation, where photocatalysts are integrated into the membrane during fabrication,[50] and (ii) immobilization on the surface of a membrane.[51] The latter approach is much more common for the fabrication of clay-based photocatalytic membranes. For the surface immobilization technique, there exist several approaches including vacuum filtration, sol dip-coating, electrospraying, chemical grafting, spin coating, and atomic layer deposition, which have all been used in the preparation of polymeric and alumina membranes.[5,50] However, so far, only sol dip coating and spin coating have been utilized for the development of clay-based photocatalytic membranes as discussed in the sections below.

3.1. Sol dip-coating

The sol-dip coating approach is one of the most promising and widely used immobilization methods for the production of clay-based photocatalytic membrane.[9,52,53] The sol used in sol dip-coating is prepared in a manner similar to that in the sol–gel method; it includes the hydrolysis of suitable precursors, polymerization of the monomers, drying of the resulting photocatalyst, and thermal treatment.[54] Thus, different starting materials can be used to produce the photocatalyst sol. Thereafter, dip-coating is used to deposit the photocatalysts on the membrane surface.

For instance, Neethu *et al.* prepared a grafted titania-pillared montmorillonite clay membrane by first preparing a flat disk membrane support and a TiO_2 sol prepared from titanium isopropoxide.[55] Thereafter, the membrane support was immersed in the TiO_2 photocatalyst sol to allow the deposition of the TiO_2 photocatalyst particles on the membrane. This approach has been successfully applied to form a continuous and uniform layer of photocatalysts on clay membranes as shown in the SEM images (Fig. 2) of titania pillared montmorillonite clay membranes prepared at pH 2 and 3. Also, an ultrafiltration layer made of TiO_2 nanoparticles can be obtained through sol-dip coating of the clay membrane.[56] Environmental scanning electron microscopy (Fig. 3) shows that the deposited layer is homogeneous on the bentonite clay membrane.

One of the very unique advantages of the sol-dip method is its ease of operation that allows for the introduction of modifiers into the sol, thereby improving the membrane's efficiency against the target contaminant.[9] For instance, in order to develop a highly efficient clay-based photocatalytic membrane with multiple functions of separation, Neethu *et al.* grafted 3-aminopropyl-triethoxysilane (APTES) to the surface of a montmorillonite membrane.[55] The grafting process gave rise to a hydrophobic membrane surface with an increased surface area (from 31 $m^2\ g^{-1}$ before grafting to 183 $m^2\ g^{-1}$ after grafting) and a firmly bonded mono-molecular layer of organosilane, which prevents the release of organic molecules into aqueous medium.[57] Thereafter, the grafted membrane support was dipped into a dispersion containing the photocatalyst (TiO_2), organic modifier (cetyltriammonium bromide, CTAB), and a binder (carboxylmethylcellulose) for a certain dip time. Then the membrane was removed, dried and sintered at 300 °C.

Typically, photocatalysts composed of only one semiconductor suffer from rapid recombination of h^+ and e^- and the limitation of a single excitation centre.[58] However, when a large band gap semiconductor such as TiO_2 is coupled with a small band gap semiconductor such as tungsten(VI) oxide (WO_3), conduction band electrons can move from the small band gap semiconductor to the large band gap semiconductor. This electron transfer process effectively reduces charge recombination, improving the overall photocatalytic efficiency.[59]

In another example, Shaban *et al.* prepared a carbon–copper co-doped TiO_2 (C–Cu–TiO_2)/natural clay membrane *via* sol dip-coating.[60] In this case, two effects could be observed: (1) a reduction of the optical band gap from 2.99 eV in the TiO_2/clay membrane to 1.77 eV in the C–Cu–TiO_2/clay membrane and (2) reduced electron–hole recombination due to the Cu dopant acting as an electron trap, which increases the photocatalytic efficiency of the co-doped membrane because more electrons and holes become available for the generation of different reactive oxygen species (ROS).

Sol dip-coating generally produces membranes with moderate porosity and a relatively thick photocatalytic layer, depending on the dip time and sol concentration. The technique allows uniform deposition of photocatalysts and offers excellent control over the surface properties by introducing modifiers or dopants. These modifications can enhance photocatalytic activity by increasing the surface area or improving light absorption. However, improper control of the withdrawal speed or sol properties may lead to cracking, uneven coatings, or reduced mechanical stability, which can compromise long-term performance under filtration pressure.

On the other hand, sol dip-coating has some limitations, which include the need for precise control of synthesis parameters, such as immersion time and especially withdrawal speed from the liquid dipping phase, to ensure uniform coating. In some cases, the deposited layer may lack sufficient mechanical strength, especially under high pressures or temperatures.

3.2. Spin coating

Spin coating is similar to sol dip-coating in that both techniques involve depositing a liquid-phase photocatalyst dispersion onto a membrane support. Spin coating has also been utilized

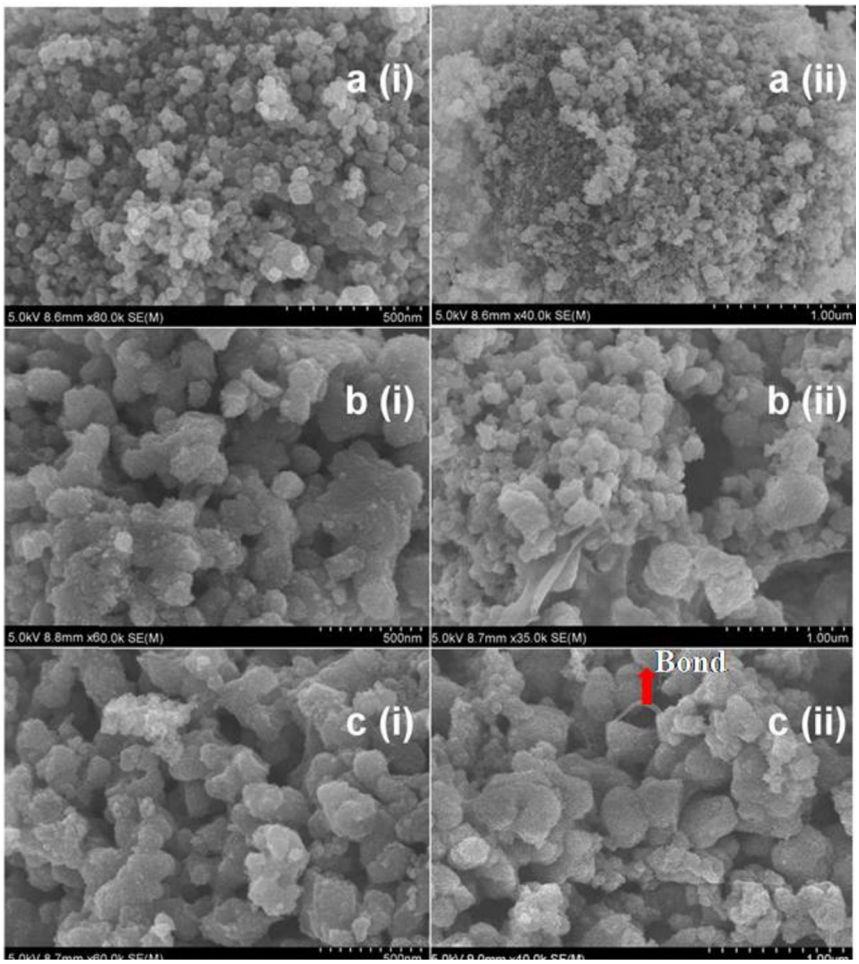

Fig. 2 Scanning electron microscope images: (a) (i) and (ii) anatase phase of pure TiO_2; (b) (i) and (ii) cross section of the titania pillared clay (TiPILC) membrane at pH 2.0; and (c) (i) and (ii) cross section of the TiPILC membrane at pH 3.5. Published under the CC BY-NC 4.0 license.[55]

for the immobilization of photocatalysts on membrane supports. In short, the photocatalyst sol is added onto the membrane surface while the membrane support is spinning at a constant rate. The centrifugal force drives the photocatalyst sol to spread by constant rotation and the solvent rapidly evaporates to produce a uniform coating layer on the membrane. Typically, there are four processes involved in spin coating: (1) rotation of the solid membrane support at high speed, (2) deposition of the photocatalyst sol on the rotating membrane, which leads to the outward flow of the photocatalyst sol (spin-up), (3) spin-off, which leads to ejection and formation of accumulations at the perimeter, and (4)

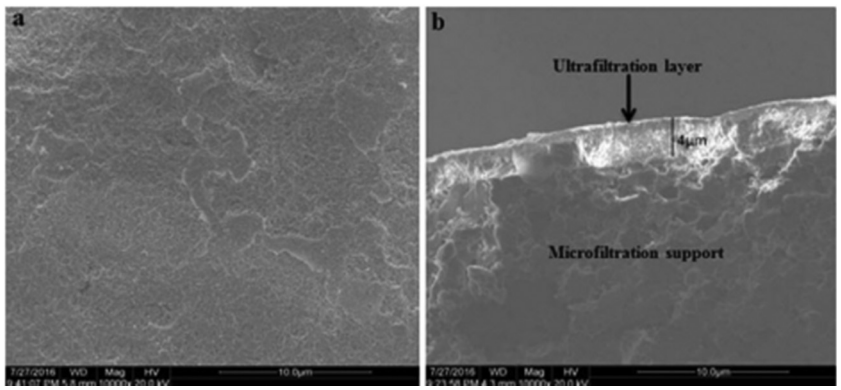

Fig. 3 Environmental scanning electron microscope micrographs of the nano-TiO_2 ultrafiltration membrane: (a) top-view and (b) cross-sectional view. Figure reprinted from ref. 56, with permission from Elsevier, Copyright 2025.

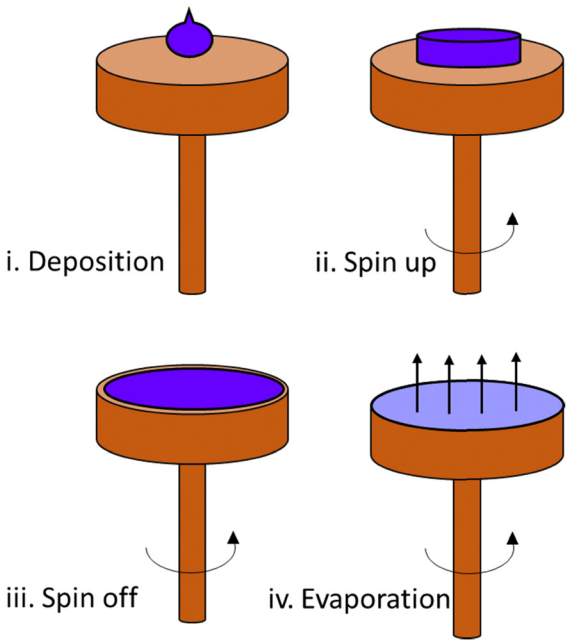

Fig. 4 Schematic diagram of the spin coating method. Published under the CC BY-NC 4.0 license.[50]

evaporation of the solution forming a thin solid membrane state[50] (Fig. 4). It is important to note that the thickness of the membrane can be controlled by the solvent evaporation rate, velocity of the spinning substrate (spin rate) and the viscosity of the coating solution.[61] For instance, Burmann *et al.* observed that the solvent evaporation rate is a significant parameter when spin coating photocatalyst membranes since fast solvent evaporation generates defective and unstable membranes.[62]

For example, a bentonite-phosphate/TiO_2 photocatalytic membrane was fabricated by spin coating[63] by first preparing a flat disk membrane support from bentonite and an unspecified micronized phosphate. Onto this support, an aqueous dispersion of TiO_2 particles and polyvinyl alcohol (PVA, used as a binder) was spin coated. According to the authors, the optimal composition (wt%) of the coating dispersion was 67% water, 30% PVA and 3% TiO_2. Indeed, SEM (Fig. 5) shows that the TiO_2 layer coated on the membrane support is homogeneous and there was good adhesion onto the membrane support. Spin coating has also been used for the fabrication of clay-based membranes[64,65] but has never been used for the fabrication of clay-based photocatalytic membranes.

Very much like some of the approaches discussed above, spin coating also has some limitations. For instance, fast solvent evaporation can result in defective and unstable membranes, and achieving uniform coatings on complex geometries or large surfaces remains challenging. Additionally, spin coating often requires precise control over multiple parameters, limiting its scalability for industrial applications.[66]

Generally, spin coating results in ultrathin photocatalyst layers with highly uniform thickness and minimal surface defects when properly controlled. The porosity of the coated layer is typically lower than that of membranes made by dip-coating, but the thinness facilitates higher light penetration and effective charge transport, enhancing photocatalytic efficiency. However, the method is sensitive to solvent evaporation rate, spin speed, and solution viscosity. Rapid evaporation can lead to structural defects, while inconsistent control over spin parameters may affect photocatalyst adhesion and membrane durability.

3.3. Other approaches towards photocatalyst/clay membranes

Spray coating is an emerging alternative that addresses some of the limitations experienced with sol-dip and spin coating. Spray coating involves spraying a photocatalyst dispersion onto a substrate using a pressurized system, allowing for more uniform coverage over irregular or larger surfaces. Spray coating offers greater flexibility in controlling the thickness of the coating and can more easily be scaled to industrial dimensions. Often, spray-coated photocatalytic membranes maintain high performance and adhesion under actual operating conditions, making spray-coat membranes a viable alternative for future applications.[67]

Another promising alternative is plasma spraying, a technique that utilizes a high-temperature plasma jet to deposit

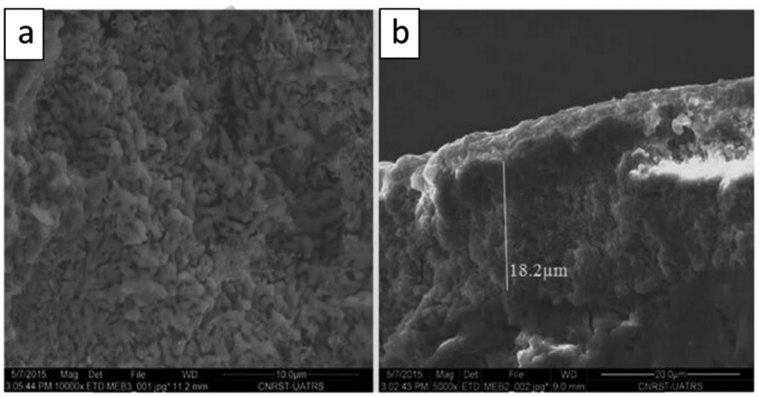

Fig. 5 Scanning electron microscope images of the bentonite-phosphate/TiO_2 membrane: (a) top view and (b) cross-sectional view. Figure reprinted from ref. 63, with permission from Elsevier, Copyright 2025.

coatings on substrates. Plasma spraying can achieve high bond strength, thicker coatings, and better resistance to mechanical and thermal stresses compared to sol dip- and spin coating.[68,69] Moreover, the technique enables the deposition of mixed-phase or composite photocatalysts, which can further enhance the performance of the photocatalytic membrane.[70] However, its application for clay-based photocatalytic membranes has not been reported to the best of our knowledge.

4. Factors influencing the performance of clay-based membranes

Clearly, there is a need for low cost and sustainable membranes, but the performance and stability of a membrane is a decisive factor. The primary factors impacting membrane performance and durability include the types of precursor material, binders, water content, pore-forming agents, sintering temperatures, and additives.[71] The influence of these factors on membrane performance is further discussed below.

4.1. Sintering temperature

Sintering plays an important role in determining the chemical transitions (*e.g.* dehydration, densification, crystallization) in the ceramics and characteristics of the specific properties such as porosity, pore size distribution, pore shape and mechanical strength of clay-based membranes.[72,73] The sintering process induces a series of physical and chemical changes through accumulation, bonding, and particle–particle interaction.[71]

In general, the sintering process can be divided into (1) pre-sintering, (2) thermolysis, and (3) densification steps. In the first step, the powders form point contact through accumulation and there are a large number of pores, while with increasing sintering temperature, the powders gradually change from point contact to neck connection, and the pores gradually shrink until a continuous dense material is formed at the last stage.[71,74] The densification of the granular compact is performed *via* thermal treatment at a temperature below the melting point of the main constituent of the membrane, increasing its strength by bonding the particles together.[33] Typically, an increase in sintering temperature promotes densification, which causes the grains between particles to grow as seen in Fig. 6, and this could contribute to the creation of more bonds between the particles resulting in membrane strengthening.[71,75]

The sintering process strongly influences the mechanical strength of the membrane by promoting the fusion and bonding of constituent particles. Thus, the sintering temperature should usually be at around three-fourth of the melting point (unfortunately the authors did not specify which melting point) of the material during membrane fabrication.[73] The higher the sintering temperature, the lower the porosity and the higher the mechanical strength.[71,77–80] At higher sintering temperatures, more liquid phase is produced on the surface of the support. The liquid phase blocks the original pores and increases the compactness in the material. Consequently, the volume of the material shrinks, which in turn results in a decrease of porosity and an increase of the bending strength.[77–80] The reason for the pore reduction is the adhesion of the liquid phase in the pore and the growth of crystalline domains upon cooling.

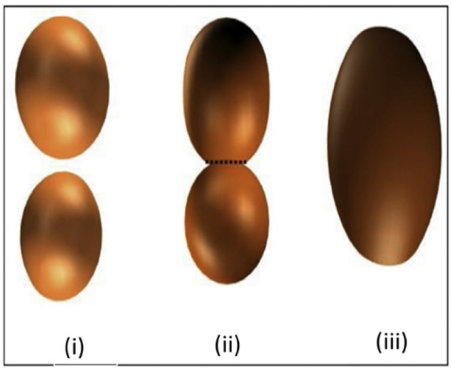

Fig. 6 (a) Schematic diagram of the grain growth mechanism: (i) particles of slightly different size in contact; (ii) neck growth by surface diffusion of the particles; (iii) grain growth occurrence. Figure reprinted from ref. 76, with permission from Elsevier, Copyright 2025.

Mohtor *et al.* studied the effect of sintering temperatures ranging from 1200 to 1500 °C in the preparation of kaolin hollow fiber membranes.[73] A reduction in membrane porosity was observed with increasing sintering temperature. Likewise, the mechanical strength was enhanced, which was attributed to the grain growth of the ceramic particles during the sintering process. In this study, higher sintering temperatures facilitated sufficient fusion and bonding between the ceramic particles, further strengthening the membrane. According to the authors, a sintering temperature of 1400 °C is the optimum sintering temperature because it resulted in a membrane with good mechanical strength, appreciable water permeation, and improved efficiency for dye filtration. Based on the result, the kaolin hollow fiber membrane sintered at temperature $\geq$1300 °C exhibits a higher mechanical strength than membranes that were sintered at $<$1300 °C.

Mouiya and co-workers prepared a clay-based membrane from a mixture of clay and 20 wt% banana peels (BP).[81] The effect of sintering temperature (900, 1000, 1100 °C) on porosity was examined as shown in Fig. 7. The membrane shows a decrease in porosity and an increase in mechanical strength as the sintering temperature increased from 900 to 1100 °C. The SEM image reveals a heterogeneous microstructure with high porosity in the sample sintered at 900 °C, whereas the number of small pores significantly decreases after sintering at 1100 °C. A decrease in apparent porosity from 47.4 $\pm$ 0.3 to 40.23 $\pm$ 0.2% as the sintering temperature increases from 900 to 1100 °C was observed. This is attributed to densification that promotes partial removal of porosity at high temperatures. Furthermore, Fig. 8 shows that excessive sintering, such as at 1200 °C, leads to the shrinking of the ceramic structure, thus resulting in a single slab of molten material.

Vasanth *et al.* reported a low-cost ceramic microfiltration membrane from kaolin, quartz, and $CaCO_3$ using a uniaxial dry

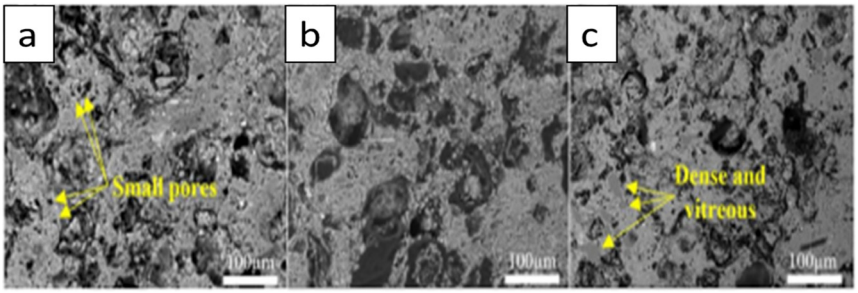

Fig. 7 Effect of sintering temperature on the microstructures of sintered samples containing 20 wt% BP: samples sintered at (a) 900 °C, (b) 1000 °C, and (c) 1100 °C. Figure reprinted from ref. 81, with permission from Elsevier, Copyright 2025.

compaction method, and observed that within the sintering temperature applied (between 900 and 1000 °C), a sintering temperature of 900 °C gave the best membrane.[72] The maximum shrinkage of the membrane was estimated to be 11%, while the particle size was in the range of 5–30 μm and the porosity of the membrane decreased with increasing sintering temperature. The flexural strength of the membrane, its chemical stability, and its water permeability increased with increasing sintering temperature. The membrane showed a maximum rejection of 85% for oil (250 mg L^{-1}) and 99% for bacteria (6×10^5 cfu mL^{-1}).

The sintering process also influences phase transitions and crystallographic properties of clay-based membranes as well as their performance. Aside from the microstructure of the membrane being affected, the sintering temperature also influences the physical appearance of the membrane. In one study, Adam and co-workers observed that increasing the sintering temperature decreases the thickness of hollow fibre ceramic membranes (HFCMs) derived from the clinoptilolite zeolitic membrane from 189 μm (T = 900 °C) to 148 μm (T = 1150 °C).[76] This reduction in thickness is linked to the densification of the ceramic particles within the membrane, as seen in the SEM micrographs (Fig. 9). Additionally, other physicochemical properties of the HFCM, such as mechanical strength and water permeability, are directly affected by the increase in sintering temperature in this study.[76] Typically, increasing the sintering temperature is expected to enhance the mechanical strength of HFCMs. However, in this case, the membrane sintered at 1150 °C exhibited the opposite trend due to structural defects, such as dead-end pores and channels. These defects compromise the overall quality of the membrane by weakening its structure. Beyond reducing mechanical strength, these imperfections also affect the membrane's performance. They allow water to pass through more quickly, shortening the contact time between the adsorbate and the adsorbent (HFCM). As a result, the membrane becomes less effective at capturing and retaining the adsorbate.

It is important to state that the sintering temperature has a tremendous influence on membrane properties and, thus, the careful selection of a suitable sintering temperature is crucial for the fabrication of a membrane with good properties (porosity, pore size, mechanical strength, *etc.*). In addition, a good compromise should be found between the sintering temperature and the former pore percentage, which refers to the initial porosity of the ceramic membrane before sintering, to achieve high water flow, high mechanical strength, and optimal ceramic membrane porosity.[82] Table 2 presents the different clay-based membranes sintered at various temperatures and their respective properties.

4.2. Pore-forming agents

The inclusion of pore formers into a membrane composition enhances both porosity and permeability. The choice and quantity of pore-forming agents are key factors in the preparation of high-quality membranes. These agents disappear completely or partially during the sintering process through mechanisms such as decomposition, evaporation, liquid phase formation or combustion.[94–96] This results in the formation of an additional porous network, modifying the pore size distribution and increasing the permeability of the membrane.[96]

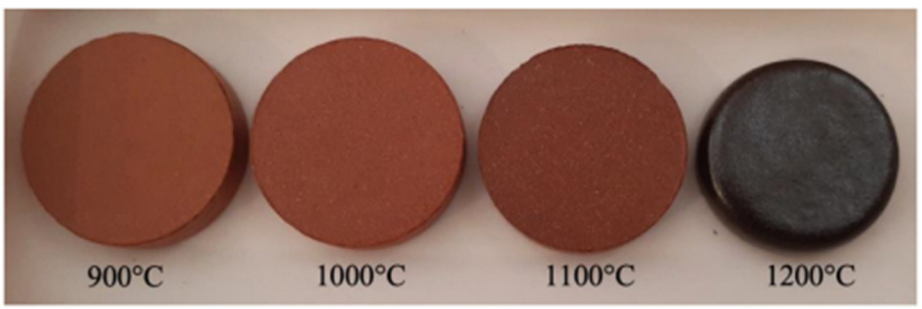

Fig. 8 Photograph of the porous ceramic sintered at different temperatures. Reprinted from ref. 81, with permission from Elsevier, Copyright 2025.

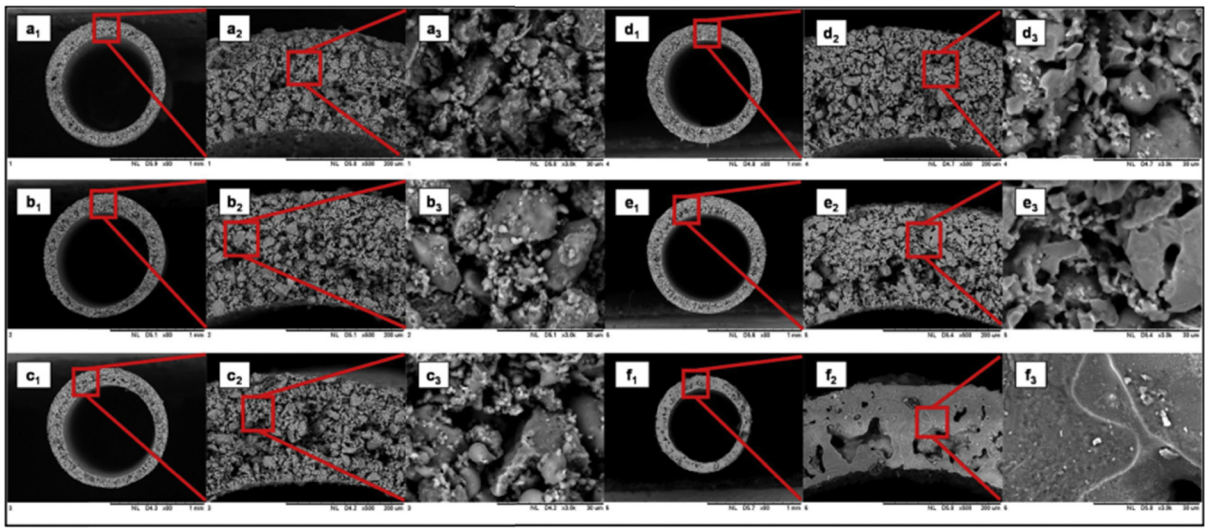

Fig. 9 SEM micrographs of the HFCMs sintered at different temperatures: (a) 900 °C; (b) 950 °C; (c) 1000 °C; (d) 1050 °C; (e) 1100 °C and (f) 1150 °C; at different magnifications: (1) 80×; (2) 500× and (3) 3000×. Figure reprinted from ref. 76, with permission from Elsevier, Copyright 2025.

Various materials, both inorganic and organic, are used as pore generators. Inorganic pore-forming agents include calcium carbonate, sodium carbonate, carbon black, or activated carbon graphite.[97,98] Organic pore-forming agents include natural fibers and polymers, such as sawdust, starch, polystyrene, and polymethyl methacrylate (PMMA).[99,100]

At elevated temperature, inorganic pore formers decompose into oxides that form a solid solution with the raw materials, promoting sintering but potentially becoming impurities that affect the purity of the crystal phase of the membrane. In contrast, organic pore formers ideally decompose completely into gas and water, which should not pollute the membrane.[71,101,102] Among the most widely used pore formers are starches and carbonates. Starch, a natural biopolymer, is usually more preferred for its low cost, ecological benefits and easy oxidation (at relatively low temperatures around 500 °C).[103] Besides starch, waste biomass like rice husk, poppy seeds, corn or wheat also holds potential for facilitating waste-to-value-added product development and for reducing the cost of clay-based membranes.[99,100,104]

Some authors have successfully produced finer pores (with an average size of around 4 μm) in ceramic membranes that are not interconnected due to discontinuous pore space channeling during the sintering process. By varying the particle size and concentration, a wide range of membrane porosity (20–70%) and average pore sizes (ranging from 0.26 to 10.21 μm) can be achieved using organic pore formers.[96,98,99]

Ahmed and Mir assessed the potential and performance of almond shells as a pore-forming agent in the preparation of a kaolin-based microfiltration membrane. The porosity and the pore diameter of the membrane was 46.45% and 0.290 μm, respectively. Additionally, the membrane displayed favorable chemical stability when exposed to both acidic and basic environments. The pure water permeability was 5.25×10^2 L m^{-2} h^{-1} bar^{-1}. The study concluded that almond shells can be economically and effectively used as a pore-forming material for the synthesis of ceramic membranes.[105]

In another study, Lu *et al.* fabricated porous mullite as supports for filtration membranes by recycling coal gangue and bauxite at sintering temperatures from 1100 to 1500 °C, using corn starch as a pore-forming agent. Without corn starch, the mullite ceramic membrane support had a low open porosity of less than 30% (Fig. 10a), which was inadequate for filtration purposes. The addition of commercial corn starch significantly increased the open porosity of the ceramic membrane to *ca.* 48%. This increase was accompanied by a gradual decrease in the bulk density and an increase in shrinkage (Fig. 10b). Furthermore, the pore size distribution of the membrane varied with different amounts of corn starch added. This adjustment led to an improved porous structure, characterized by larger pores and increased open porosity. The enhancement occurred as the larger-sized corn starch particles burned away during sintering, creating more voids compared to membranes without corn starch. The microstructure of the mullite ceramic membrane, influenced by the pore-forming agent, is illustrated in the SEM images in Fig. 11.[106]

Chakrabortz *et al.* studied the impact of varying compositions of sawdust particles (a natural pore-former) on low-cost ceramic membranes.[96] Reducing the amount of sawdust from 8 to 1 wt% led to a decrease in membrane porosity from 28.47% to 21.69%. The membranes had an average pore size from 0.45 to 1 μm, which falls within the typical range for microfiltration membranes (0.1–10 μm). These membranes can be used for heavy metal removal, oil–water separation, or removing microbes to produce potable water.

In 2017, Obada and co-workers developed a low-cost macroporous ceramic membrane from natural kaolin. The authors incorporated high-density polyethylene (PHDPE) powder as a pore-forming agent, varying its content from 5 to 20% to create macroporous membranes.[107] SEM images (Fig. 12) show that the addition of the pore former PHDPE led to an increase in porosity, pore size, and pore connectivity. This effect was attributed to the increase in the number of interconnected

Table 2 Performance comparison of ceramic membranes sintered at various temperatures and their properties

Membrane type	Binder	Sintering temperature (°C)	Porosity (%)	Pore size (μm)	Water permeability	Mechanical strength (MPa)	Ref.
Hollow fibre ceramic membrane	Calcium carbonate	1050	55	N/A	228.25 L h^{-1} m^{-2} bar^{-1}	54.20	76
Fly ash, kaolin and dolomite ceramic membrane	Sodium metasilicate (pentahydrate)	900	46.3	0.62	450 L h^{-1} m^{-2} bar^{-1}	49.4	77
Ceramic membranes from fly ash and kaolin	N/A	900	42.7	0.885	1010 L h^{-1} m^{-2} bar^{-1}	43.6	83
Kaolin microfiltration membrane	N/A	1250	27	0.73	20 L h^{-1} m^{-2} bar^{-1}	28	84
Kaolin and calcite membrane	N/A	1150	50.50	4	N/A	28	85
Porous mullite ceramic membrane	PVA	1450	31.60	0.62	N/A	99	86
High-aluminium fly ash ceramic membrane	PVA	1300	> 30	1.2	N/A	> 30	78
Mullite hollow fibre membrane	poly-ethersulfone (PES)	1250	50.50	0.61	1286 L h^{-1} m^{-2} bar^{-1}	55.80	44
Porous kaolin membrane support	Polyethersulfone (PESf)	1200–1500	5.20–57.80	0.35–4.25	N/A	15.78–63.10	87
Micro-structured alumina hollow fibre membrane	Polyethersulfone (PESf)	1455	N/A	< 0.20	664–1088 L h^{-1} m^{-2} bar^{-1}	88.20–116.50	88
Bentonite based nano-TiO_2 ultrafiltration membrane	PVA	950	N/A	0.009–0.012	16.08 L h^{-1} m^{-2} bar^{-1}	N/A	56
Disc membrane		900	41	1.78	2.88×10^{-2} L h^{-1} m^{-2} bar^{-1}		89
Ball clay-based hollow fibre membrane	N/A	1000	41	0.31	7.69×10^{-9} L h^{-1} m^{-2} bar^{-1}	50	90
Metakaolin-based ceramic hollow fibre membrane (CHFM)	Polyethersulfone (PESf)	1500	12	0.007	N/A	225.80	87
Natural/Assam kaolin based ceramic microfiltration membrane	Sodium metasilicate Boric acid Sodium carbonate		34.50	2.28	6.12×10^{-9} m sPa^{-1}	7.1	91
China clay based membrane	Polyvinyl alcohol	900	42	0.18 nm	3.24×10^{-4} L h^{-1} m^{-2} bar^{-1}	50.65	92
Bentonite, talc, sodium borate, and carbon black	Polyethylene glycol	1000	34	0.65–1.25	1.75×10^{-5} L h^{-1} m^{-2} bar^{-1}	58	93

pores created by the burnout of the pore former, resulting in higher permeability. The impact of increasing the pore former content on the apparent porosity and water absorption of the sintered clay-based membranes is clearly illustrated in Fig. 13, showing an increase in porosity and water absorption with higher pore former content.[107]

As demonstrated above, the properties of clay-based membranes, such as pore size, porosity, and mechanical strength, are significantly affected by the type, composition and amount of pore-forming agents used during fabrication. By optimizing these parameters, researchers can achieve the desired combinations of pore size and porosity in (clay-based) membranes, leading to a better understanding and control of the membrane characteristics. This knowledge is crucial for optimizing the performance and applicability of low-cost clay membranes in various filtration and separation processes.

4.3. Binders

In the production of clay-based ceramic membranes, binders are utilized to strengthen the membrane by creating bridges between particles. Additionally, the binder contributes to plasticity and assists in green body formation, but is usually removed as much as possible during the sintering process.[33,108]

Several raw materials used in membrane fabrication, such as clay, alumina, and titanium dioxide, exhibit poor fluidity and formability.[71] Using these materials alone can result in issues like uneven density distribution, cracks, and delamination after sintering. Therefore, adding a suitable binder is essential to adjust the forces of attraction between the powder particles, thus enhancing their rheological properties and plasticity, making molding easier while maintaining the desired shape.[33,71,109] Cellulose derivatives, including MC,[110] carboxymethyl cellulose (CMC),[111] PVA,[112] or hydroxypropyl methylcellulose (HPMC),[71] are commonly used as binders in membrane fabrication. Other low-cost binders like starch from corn, wheat, and potato have also been employed.[18,71,113] The addition of these binders to the raw materials alters the performance of the membrane support.

Singh *et al.* used kaolin, quartz, and calcium carbonate as raw materials, and carboxymethyl cellulose (CMC) as a binder to prepare tubular porous clay-based membranes *via* extrusion and sintering at 950 °C.[114] Increasing the CMC content from 0 to 3 wt% led to a decrease in the porosity of the membrane from 48 to 36%, while the bending strength increased from 21 to 38 MPa. The study demonstrates that a higher CMC content resulted in reduced porosity but increased the bending strength and water flux of the membrane. The increase in water flux could be attributed to the larger pore size of the membrane as the binder content increased (Fig. 14a and b).

Boussemghoune *et al.* investigated the influence of other organic binders including gelatin, methocel, ethylene glycol (EG), and polyethylene glycol (PEG) on the morphology of ceramic membranes made from materials such as kaolin.[115] Kaolin was chosen due to its specific properties and cost-effectiveness. SEM reveals that using gelatin as a binder results in large holes in the membrane after sintering, while the

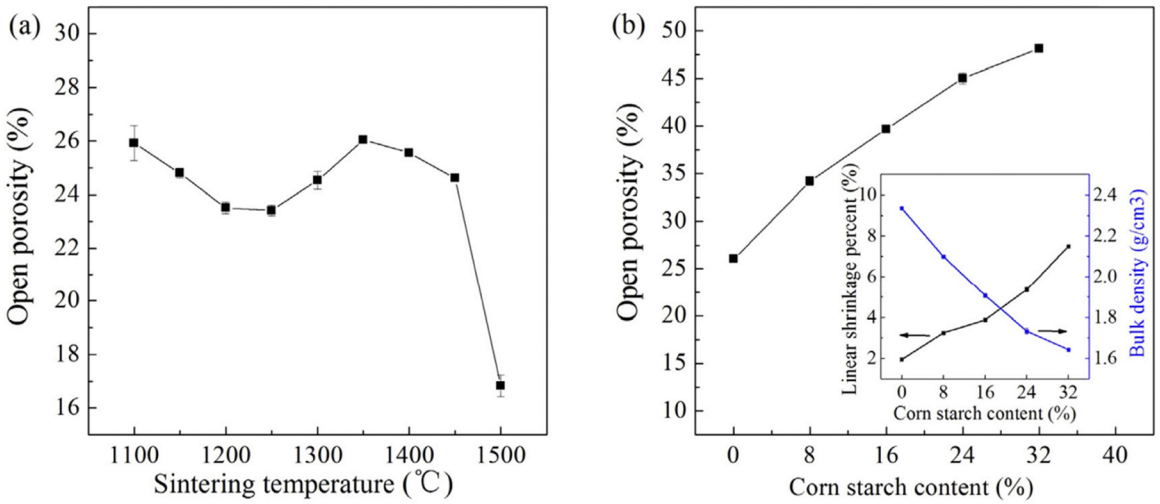

Fig. 10 Open porosity of the mullite ceramic membrane supports: (a) without corn starch addition after sintering at 1100–1500 °C, and (b) with the addition of various contents of corn starch after sintering at 1350 °C (the inset shows the effect of corn starch content on the bulk density and shrinkage of the membrane). Figure reprinted from ref. 106, with permission from Elsevier, Copyright 2025.

membrane produced with methocel shows a uniform and homogeneous pore structure due to the strong deflocculating properties of methanol.[115] The authors attributed the differences observed with these organic binders to variations in their chemical structure and properties, such as polarity, molecular weight, and polymer chain length, which significantly influence the overall microstructure of the membrane support.

The presence of binders in clay-based membranes plays a key role.[116] It is important to carefully add and optimize binder content to achieve efficient membrane performance and functionality for specific applications[33,71] but at the same time the characteristics of a specific binder must be matched to the overall system.

5. Design of experiment

The fabrication of clay-based membranes is influenced by variables such as particle size, additives, processing, *etc.* Optimization of these parameters and variables is expensive because it typically entails numerous trial-and-error approaches.[117] Apart from being expensive, only one factor is varied at a time while others are fixed and this neglects the interaction among all factors in the overall process.[118] This makes conventional trial-and-error approaches time-, material-, cost-, and labour-intensive. In an attempt to solve this enormous issue (which is prevalent in materials research in general) a number of recent studies have design of experiments (DOE) software to reduce the number of experiments, and to determine a response value for any selected variable belonging to the investigated experimental domain.[119,120] In DOE, the Plackett–Burman design (PBD) is a very effective screening method to identify the most significant factors that influence a process using only a few experimental runs.[121,122] In addition, the response surface methodology (RSM) from DOE has been widely used to assess the significance of several independent parameters for the response variable and their interaction effects using the lowest number of experiments possible.[123] The RSM has advanced the field of membrane science due to the development of statistical models which are helpful during

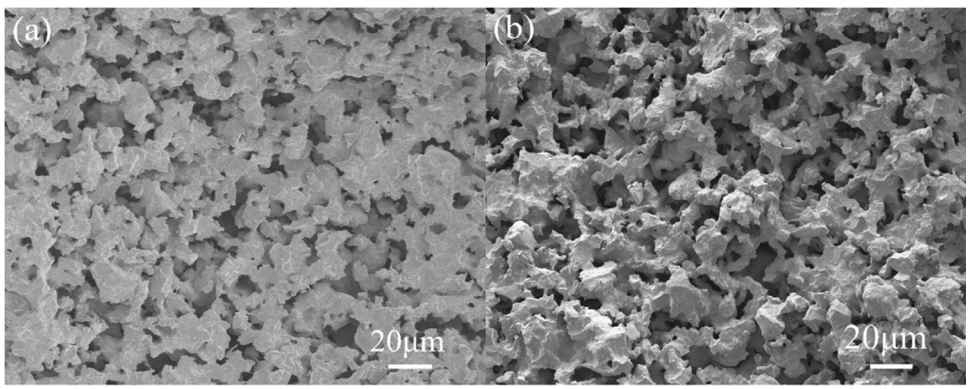

Fig. 11 Scanning electron microscope images of fracture surfaces of the mullite ceramic membrane supports sintered at 1350 °C with (a) 16 wt% and (b) 32 wt% corn starch addition. Figure reprinted from ref. 106, with permission from Elsevier, Copyright 2025.

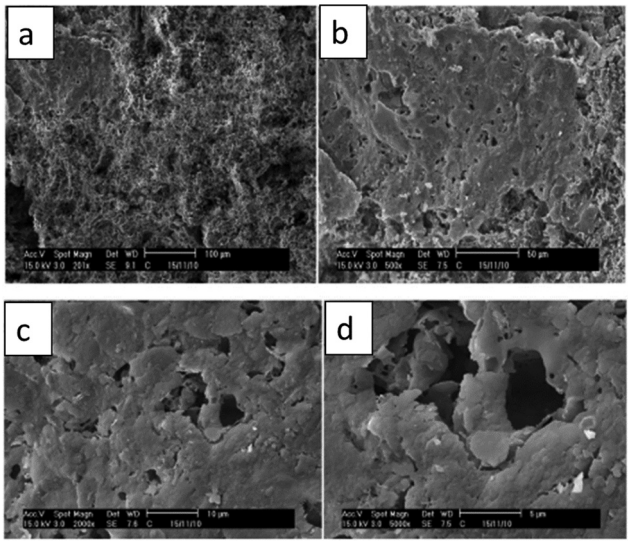

Fig. 12 Scanning electron microscope images of sintered membranes with HDPE as the pore former at 20 wt%: (a) 201×, (b) 500×, (c) 2000×, and (d) 5000×. Figure reprinted from ref. 107, with permission from Elsevier, Copyright 2025.

the simulation and optimization process to generate cost-effective and efficient process designs.[124,125] Table 3 shows the operational conditions employed in experimental studies for the preparation of clay-based photocatalytic membranes.

Baih *et al.* employed the PBD to evaluate and screen the effects of sintering temperature (ST), particle size (PS), starch content (SC), and heating rate (HR) on the porosity and mechanical strength of a clay-based ceramic membrane.[120] The regression model and analysis of variance (ANOVA) show that the ST had the strongest influence on the mechanical strength, followed by SC, PS and HR. In contrast, only ST and SC had major effects on the porosity of the membrane. Hence, an increase in ST decreases the porosity and increases the mechanical strength of the membrane. This effect could be attributed to the strong influence of temperature on the melt formation and invariably on the sintering process. However, an increase in SC was accompanied by an increase in the membrane porosity. The authors assigned this effect to pore formation during the burning out of the starch at around 500 °C.[100] Baih *et al.* further optimized the significant factors (ST and SC) obtained from PBD with RSM using central composite design (CCD). RSM-CCD showed the combined effect (interaction) of ST and SC on the porosity and mechanical strength of the membrane. Hence, the optimized predicted response (porosity: 38.8% and mechanical strength: 12 MPa) for the membrane was achieved with SC at 4% and ST at 1014.4 °C.[120]

Bose *et al.* investigated the effect of binder content (sodium metasilicate (SM) and boric acid (BA)) and preparation pressure on membrane porosity and flexural strength using the CCD of RSM.[116] High pressure and high BA content were the most significant individual parameters to produce a membrane with high flexural strength. On the other hand, there were no significant interactions between the independent parameters with each other to enhance the membrane porosity. However, there were obvious individual impacts of each parameter as the maximum porosity was obtained at a preparation pressure of 7.84 MPa and 5% of binder content. Similar to what has been observed for the effects on flexural strength, the amount of BA has a major effect on the membrane porosity, much more so than the sodium metasilicate content. Therefore, the optimum membrane fabrication conditions as generated by the RSM-CCD were obtained at 9.81 MPa and 7.5% of SM and BA each with a desirability function of 0.97.[116]

Aside from the use of RSM for the optimization of process variables in membrane fabrication, some studies have explored its use in the optimization of membrane applications. For instance, Ahmed *et al.* employed the Box-Behnken design (BBD) in RSM for the optimization of Fe removal using a combined oxidation–microfiltration process.[117] The optimal input conditions for the responses (Fe rejection and permeate flux) were determined using a second-order polynomial equation. The BBD responses showed

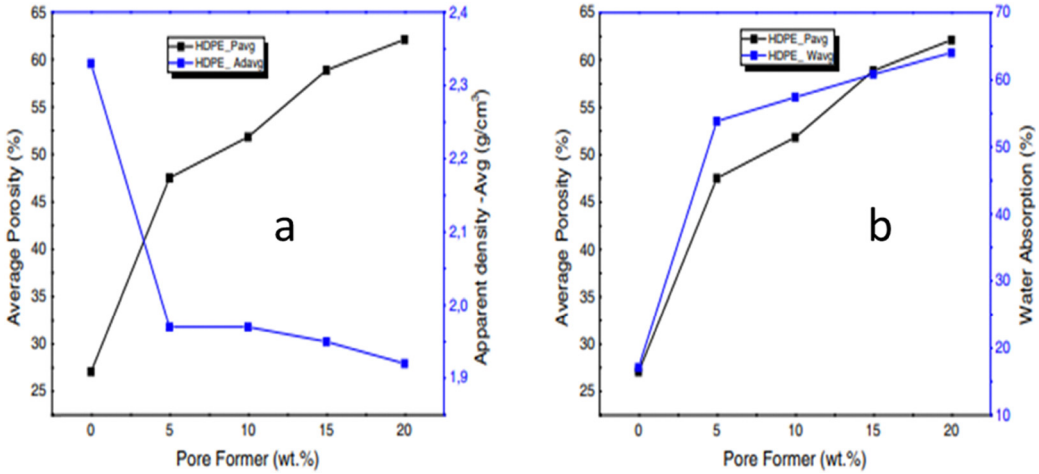

Fig. 13 (a) Porosity and apparent density of sintered membranes and (b) porosity and water absorption of sintered membranes with varying pore former content. Figure reprinted from ref. 107, with permission from Elsevier, Copyright 2025.

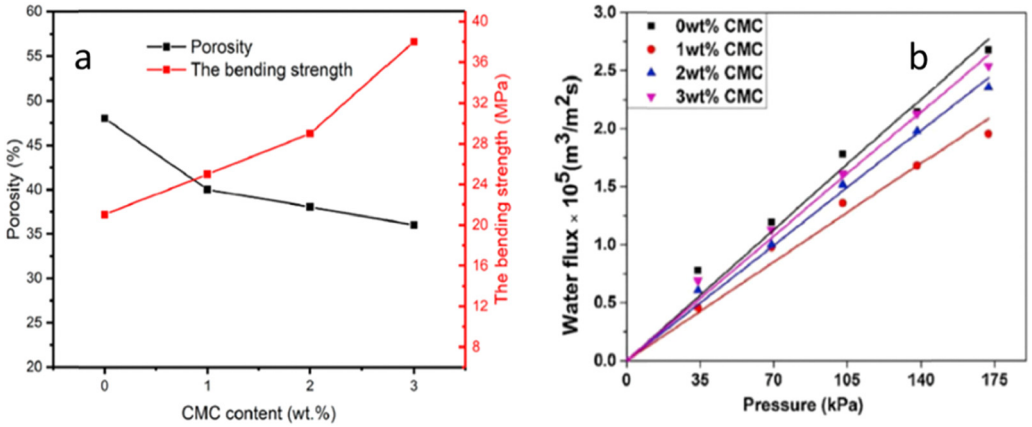

Fig. 14 Effect of binder content on (a) porosity and bending strength and (b) water flux of the ceramic membrane. Figure reprinted from ref. 114, with permission from Elsevier, Copyright 2025.

Table 3 Summary of operational conditions used in experimental studies on clay-based photocatalytic membranes

Membrane type	Sintering temperature (°C)	Heating rate (°C min^{-1})	Mechanical strength (MPa)	Porosity (%)	Membrane thickness (mm)	Density (g cm^{-3})	Ref.
Clay ceramic membrane	900–1200	1–10	11–19	15–42	—	—	120
Kaolin microfiltration membrane	850	3	150	46	5	—	117
Tubular ceramic membrane	550–850	1	7–12	10–28	10	—	116
Anorthite-based ceramic membrane	900–1200	5	—	48–52	—	2.5	126
Clay-based ceramic membrane	1150–1250	5	30	0.9–7.9	—	1.9–2.2	127

that the maximum Fe rejection and maximum flux values were 83.02% and 4.75 L h^{-1} m^{-2} bar^{-1} respectively. The result from the BBD optimization shows that the membrane has good potential for the removal of iron from groundwater.

It is worth noting that, even though some studies have employed RSM for the optimization of ceramic membrane fabrication and application, very few studies have used this important tool for the preparation and application of clay-based photocatalytic membranes. Considering the advantages of RSM in experimental design, we recommend that more studies should employ this vital technique for the identification of optimum parameters and their interaction effect for the fabrication of efficient and effective clay-based membranes for water and wastewater treatment.

6. Applications of clay-based photocatalytic membranes

Despite the intriguing benefits of clay such as better thermal, chemical and mechanical stability in comparison to polymeric substances, only few studies have utilized clay-based photocatalytic membranes for water treatment.[117] This section highlights some interesting recent applications of clay-based photocatalytic membranes.

6.1. Removal of organic and inorganic pollutants

The removal of organic pollutants is one of the fundamental missions in water treatment because of their ability to bioaccumulate in fatty tissues, long-range transportation, persistent nature, and toxicity even at low concentrations.[128] Their toxicities are often well known, and their presence in drinking water above a particular threshold can seriously endanger human health.[129] For the removal of these contaminants, a variety of methods have been used, such as biological treatment, advanced oxidation processes, electrochemical oxidation, membrane technologies, and adsorption.[130] Unfortunately, each of these approaches has its own limitations or drawbacks.[131] In an effort to overcome these constraints, techniques combining two or more technologies have gained increasing attention. Recently, this has resulted in the simultaneous application of photocatalysis and membrane technology known as photocatalytic membranes.[132,133] Photocatalytic membranes reject contaminants *via* membrane filtration and degrade them by photocatalysis at the same time. For instance, in a typical dye degradation process by clay-based photocatalytic membranes, the process involves adsorption of dye molecules near photocatalyst sites, followed by photoinduced generation of ROS under light irradiation. These ROS oxidize the dye molecules, leading to cleavage of chromophoric groups and subsequent mineralization into CO_2 and H_2O. The membrane's structure and surface chemistry influence how effectively this sequence occurs, depending on photocatalyst loading, light exposure, and membrane porosity. While rejection and degradation take place in the same step, reactive oxygen species (ROS, such as hydroxyl radicals, $^{\bullet}OH$, holes, h^+, and superoxide radicals $^{\bullet}O_2^-$) are generated on the photocatalyst surfaces when irradiated. These ROS are key to the degradation of organic pollutants.[7]

For example, in the purification of seawater by C–Cu–TiO_2/clay membranes,[60] clay membranes without photocatalyst coating

only have 4.2% removal efficiency for total organic carbon (TOC). However, when a photocatalyst is present on the membrane, 4 h of irradiation with UV and natural sunlight yields 83.1% and 99.5% TOC removal efficiency, respectively. Moreover, the mineralization, that is the complete degradation of the organic contaminants to water and carbon dioxide, reached 81.9% and 93.2% respectively, under the same condition (*i.e.* 4 h irradiation of UV and sunlight). The result can be attributed to the presence of a highly active photocatalyst on the surface of the membrane, which releases radicals capable of degrading and mineralizing organic compounds in polluted seawater.

Membranes also play a fundamental role in the removal of contaminants. It is worth noting that the retention efficiency of membranes is crucial for the effective removal of organic contaminants, and they are directly related to volumetric flux.[134] For instance, a TiO_2 ultrafiltration membrane supported on natural bentonite was used for the removal of the dye Direct Red 80 (DR-80).[63] As the feed concentration increased from 25 to 100 ppm, the retention of the dye increased from 80 to 98%, while a flux decline was observed. In addition to feed concentration and flux, filtration time can also influence contaminant rejection, particularly in cases where the membrane exhibits adsorptive properties. For example, Bhattacharya *et al.*[16] reported a 99% removal of ciprofloxacin within 60 min of operation, which later decreased to 90% at 90 min of operation, suggesting that the membrane acted as an adsorptive membrane.

Photocatalytic membranes can be regarded as charged membranes (because they generate charges when exposed to light due to their surface properties and the presence of photocatalytic materials). As a result, the removal of organic contaminants using photocatalytic membranes may also involve electrostatic interactions. It has indeed been reported that a membrane surface where an electrostatic repulsion between the membrane and the contaminant is present is favorable for filtration.[135] For example,[56] methylene blue (MB), a cationic dye, was effectively rejected by a bentonite clay membrane in acidic medium while DR-80 and acridine orange (AO), both of which are anionic dyes, were rejected by the same membrane in alkaline medium. As the point of zero charge of the membrane is pH 5.7, the membrane was positively charged at pH values below 5.7, which leads to the electrostatic rejection of MB (which is also positively charged). At pH above 5.7, an analogous electrostatic repulsion between the negatively charged membrane surface and the negatively charged dyes DR-80 and AO leads to their rejection. This study shows that pH had a great effect on the removal efficiency of the dyes, as the surface of the clay photocatalytic membrane changed with pH values, thus presenting a significant influence on the adsorption capacity of the organic contaminants.

Furthermore, the use of clay membranes with or without a photocatalyst present enables the targeting of positively charged species such as methylene blue and heavy metal ions; this is due to the high abundance of negatively charged active sites in the clay.[136] Although some of the hydroxyl groups on the surface of the clay membrane might be removed during calcination, the bulk and the surface of calcined clay membranes still retain negatively charged sites due to the presence of Si–O and Al–O bonds, making them highly attractive candidates for targeting (heavy) metals.

Titanium pillared clay membranes fabricated between 300 and 600 °C were utilized for the removal of MB with ~100% rejection.[137] Among different clay-based membranes, halloysite, a naturally occurring nanotubular clay mineral, was investigated for its unique structural advantages. The high photocatalytic degradation efficiency of a halloysite-TiO_2 membrane was attributed to its high surface area, large pore volume offered by the halloysite nanotube structure and the good chemical and mechanical stability of the clay, which contributed to enhancing the degradation reaction.[138] However, halloysite possesses natural, inherent TiO_2 which would make further addition of TiO_2 unnecessary and time-consuming.

6.2. Antifouling performance

The fundamental disadvantage that prevents the adoption of membrane filtration in long-term practical applications is membrane fouling.[139] When particles or macromolecules deposit or adsorb onto membrane pores, the holes of the membrane become smaller or clogged. This is followed by extensive fouling. There are many types of foulants, including biological (bacteria, fungi), colloidal (clay, flocs), scaling (mineral precipitates), and organic (oil, polyelectrolytes, and humic) substances that can block membrane pores and, in some cases, induce permanent fouling. As a result, there are frequent filtration shutdowns and the water produced is of lower quality.[140] Efforts to reverse the trend of fouling have involved the use of chemicals for cleaning the membranes or outright replacement of the membranes altogether. These methods increase the cost of the entire filtration operation and ultimately reduce membrane lifespan.[140] A sustainable method to avoid membrane fouling and increase the life cycle is – again – the use of photocatalytic membranes.[5]

With photocatalysts on a membrane, the membranes can both be anti-fouling and self-cleaning. Clay-based photocatalytic membranes mitigate fouling through a synergistic combination of surface chemistry and photocatalytic activity.[13,21] The hydrophilic and negatively charged nature of natural clays reduces the adhesion of organic contaminants, while the embedded photocatalysts generate reactive oxygen species (ROS) under UV or visible light irradiation. These ROS oxidize and degrade adsorbed foulants directly on the membrane surface, thereby reducing irreversible fouling.[141] Additionally, clay incorporation can suppress electron–hole recombination in the photocatalyst, enhancing ROS generation and sustaining antifouling performance over repeated cycles.[6]

This integrated approach also minimizes secondary pollution by preventing the leaching of nanoscale particles. Upon light activation, the photocatalysts produce highly reactive radicals that *in situ* mineralize organic pollutants on the membrane surface into CO_2, H_2O, and inorganic ions (Fig. 15). Thus, photocatalytic membranes enable simultaneous chemical oxidation and physical separation of trace

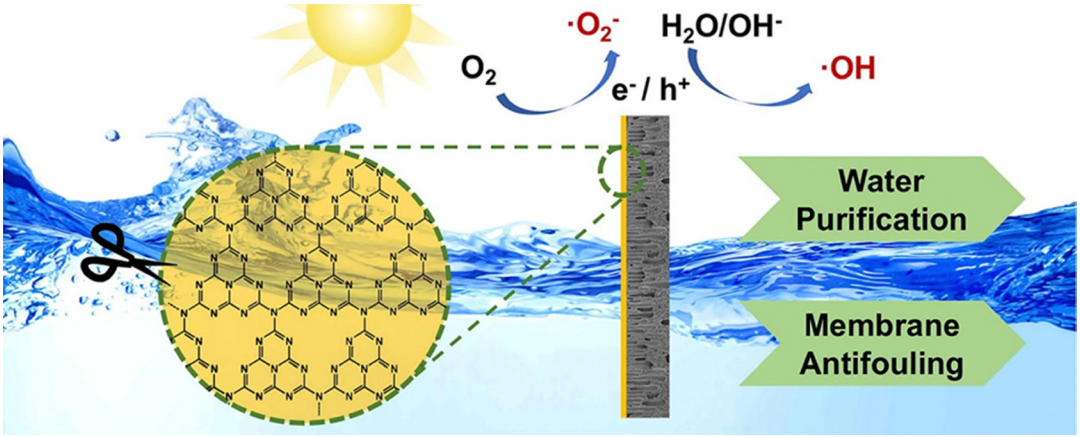

Fig. 15 Schematic illustration of the dual purpose of clay-based photocatalytic membranes.

contaminants within a single unit. The direct contact between the photocatalytic surface and foulants enhances self-cleaning behavior, and visible-light-driven photocatalysts are especially attractive due to their ability to harness abundant solar energy for sustainable water treatment applications.[47]

Functionalization of photocatalytic membranes can enhance the antifouling potential of clay-based photocatalytic membranes.[142] For example, montmorillonite-TiO_2 composite membranes were used to remove organic compounds from water. The addition of the clay resulted in the enhancement of photocatalysis when compared with the neat TiO_2 membrane without the clay.[143] Similarly, Domenzain-Gonzalez *et al.* used a Mexican natural zeolite (MNZ) to form a mesoporous cylindrical membrane.[144] The addition of MNZ to the photocatalytic membrane enhanced the removal of the reactive black 5 (RB5) dye and improved the discoloration. In addition, the membrane was suitable for reuse up to 12 cycles maintaining 88.3% dye removal. However, the proportion of zeolite in photocatalytic membranes should be optimized, because excessive incorporation of zeolite into the photocatalytic membranes could also decrease the oxidation efficiency of the photocatalytic membrane as a result of pores.[140]

7. Conclusion and future perspectives

It has been well established over the years that membrane technology for large scale water treatment has significant advantages over other water treatment technologies such as adsorption, filtration, coagulation and flocculation. However, membrane fouling is still a major challenge in membrane applications for water treatment. The incorporation of semiconductors into membranes during membrane production enhanced their performance and contributed to fouling mitigation *via* photocatalysis.

Of the two major membrane types, *i.e.*, polymeric and ceramic membranes, ceramic membranes are known to have several advantages as discussed in this review. Unfortunately, one of the drawbacks in the application of ceramics is the high cost of raw materials, which increases the overall production cost. To circumvent this, natural clays have been extensively used for the preparation of low-cost ceramic membranes but their use in the development of photocatalytic ceramic membranes is still limited. Despite the outstanding properties of natural clays, including that they are a renewable resource, low cost, environmentally benign, hydrophilic in nature, relatively abundant in nature, and have good mechanical strength, only a few studies have reported their use in the fabrication of photocatalytic membranes *via* sol-dip coating. Yet, there are no deep-dive studies to optimize the appropriate immersion time for highly efficient clay-based photocatalytic membranes. On the other hand, several routes such as chemical vapor deposition, vacuum filtration, liquid phase deposition, *in situ* condensation, phase inversion, *etc.* have been employed for the preparation of other ceramic (alumina, zirconia and titania) and polymeric photocatalytic membranes. More research should focus on the use of these synthesis routes for producing clay-based photocatalytic membranes.

Furthermore, the number of more selective clay-based membranes for ultra- and nano-filtration (UF and NF) applications is still limited because of the existence of unwanted compounds such as calcite, dolomite, quartz, amorphous silicate and organic matter in natural clay. The presence of these compounds in excessive amounts generates large pore sizes and cracks especially during the preparation of thinner membrane layers necessary for UF and NF. Hence, the purification of the clay material prior to its use in membrane preparation should be considered a key factor in order to develop clay-based membranes with thinner layers, enhanced properties, and high filtration performance.

Additionally, large scale fabrication of clay-based photocatalytic membranes could still be a challenge for their practical application for water treatment. This is because it is very tedious to manually optimize the various variables required for the successful preparation of clay-based photocatalytic membranes. Therefore, future studies on the preparation and application of clay-based photocatalytic membranes for water purification should explore the use of design of experiment (DOE) to optimize the significant factors during membrane

preparation and photocatalytic processes of different photocatalysts. This could help reduce the cost of labour, and further enhance the simulation and optimization process to generate cost-effective and efficient process designs suitable for large scale application.

Overall, it is undoubtedly clear that the future of clay-based photocatalytic membranes in water purification is promising as they offer significant advantages over polymeric and other ceramic membranes. From our literature search, there is scarcity of data on the application of clay-based photocatalytic membranes for water treatment. In addition, an in-depth understanding of the fabrication and removal mechanism of contaminants using clay-based photocatalytic membranes is still required in order to successfully deploy them for real-life water treatments.

Data availability

The article under question is a review, hence no original data are to be reported.

Conflicts of interest

There are no conflicts to declare.

Acknowledgements

The authors acknowledge, with thanks, the support of the Alexander von Humboldt Foundation to C. G. O. in the development of this manuscript.

References

1 S. G. Michael, I. Michael-Kordatou, S. Nahim-Granados, M. I. Polo-López, J. Rocha, A. B. Martínez-Piernas, P. Fernandez-Ibanez, A. Agüera, C. M. Manaia and D. Fatta-Kassinos, Investigating the impact of UV-C/H_2O_2 and sunlight/H_2O_2 on the removal of antibiotics, antibiotic resistance determinants and toxicity present in urban wastewater, *Chem. Eng. J.*, 2020, **388**, 124383.

2 I. Sirés and E. Brillas, Remediation of water pollution caused by pharmaceutical residues based on electrochemical separation and degradation technologies: a review, *Environ. Int.*, 2012, **40**, 212–229.

3 G. Wang, S. Chen, H. Yu and X. Quan, Integration of membrane filtration and photoelectrocatalysis using a TiO_2/carbon/Al_2O_3 membrane for enhanced water treatment, *J. Hazard. Mater.*, 2015, **299**, 27–34.

4 P. J. Alvarez, C. K. Chan, M. Elimelech, N. J. Halas and D. Villagrán, Emerging opportunities for nanotechnology to enhance water security, *Nat. Nanotechnol.*, 2018, **13**, 634–641.

5 M. Zhang, Y. Yang, X. An and L.-A. Hou, A critical review of g-C_3N_4-based photocatalytic membrane for water purification, *Chem. Eng. J.*, 2021, **412**, 128663.

6 C. Li, N. Zhu, S. Yang, X. He, S. Zheng, Z. Sun and D. D. Dionysiou, A review of clay based photocatalysts: Role of phyllosilicate mineral in interfacial assembly, microstructure control and performance regulation, *Chemosphere*, 2021, **273**, 129723.

7 M. O. Alfred, C. G. Olorunnisola, T. T. Oyetunde, P. Dare, R. R. Vilela, A. de Camargo, N. A. Oladoja, M. O. Omorogie, O. D. Olukanni and A. D. J. Motheo, Sunlight-driven photocatalytic mineralization of antibiotic chemical and selected enteric bacteria in water via zinc tungstate-imprinted kaolinite, *Green Chem. Lett. Rev.*, 2022, **15**, 705–723.

8 S. O. Ganiyu, E. D. Van Hullebusch, M. Cretin, G. Esposito and M. A. Oturan, Coupling of membrane filtration and advanced oxidation processes for removal of pharmaceutical residues: A critical review, *Sep. Purif. Technol.*, 2015, **156**, 891–914.

9 S. Leong, A. Razmjou, K. Wang, K. Hapgood, X. Zhang and H. Wang, TiO_2 based photocatalytic membranes: A review, *J. Membr. Sci.*, 2014, **472**, 167–184.

10 R. Molinari, C. Lavorato and P. Argurio, Recent progress of photocatalytic membrane reactors in water treatment and in synthesis of organic compounds. A review, *Catal. Today*, 2017, **281**, 144–164.

11 S. Karki, G. Hazarika, D. Yadav and P. G. Ingole, Polymeric membranes for industrial applications: Recent progress, challenges and perspectives, *Desalination*, 2023, 117200.

12 L. Chen, P. Xu and H. Wang, Photocatalytic membrane reactors for produced water treatment and reuse: Fundamentals, affecting factors, rational design, and evaluation metrics, *J. Hazard. Mater.*, 2022, **424**, 127493.

13 A. Oun, N. Tahri, S. Mahouche-Chergui, B. Carbonnier, S. Majumdar, S. Sarkar, G. C. Sahoo and R. B. Amar, Tubular ultrafiltration ceramic membrane based on titania nanoparticles immobilized on macroporous clay-alumina support: elaboration, characterization and application to dye removal, *Sep. Purif. Technol.*, 2017, **188**, 126–133.

14 C. Li, W. Sun, Z. Lu, X. Ao and S. Li, Ceramic nanocomposite membranes and membrane fouling: A review, *Water Res.*, 2020, **175**, 115674.

15 P. Bhattacharya, S. Majumdar, S. Bandyopadhyay and S. Ghosh, Recycling of tannery effluent from common effluent treatment plant using ceramic membrane based filtration process: a closed loop approach using pilot scale study, *Environ. Prog. Sustainable Energy*, 2016, **35**, 60–69.

16 P. Bhattacharya, D. Mukherjee, S. Dey, S. Ghosh and S. Banerjee, Development and performance evaluation of a novel CuO/TiO_2 ceramic ultrafiltration membrane for ciprofloxacin removal, *Mater. Chem. Phys.*, 2019, **229**, 106–116.

17 E. Alventosa-deLara, S. Barredo-Damas, M. Alcaina-Miranda and M. Iborra-Clar, Ultrafiltration technology with a ceramic membrane for reactive dye removal: optimization of membrane performance, *J. Hazard. Mater.*, 2012, **209**, 492–500.

18 S. Mestre, A. Gozalbo, M. Lorente-Ayza and E. Sánchez, Low-cost ceramic membranes: A research opportunity for

industrial application, *J. Eur. Ceram. Soc.*, 2019, **39**, 3392–3407.

19 C. O. Mgbemena, N. O. Ibekwe, R. Sukumar and A. R. Menon, Characterization of kaolin intercalates of oleochemicals derived from rubber seed (Hevea brasiliensis) and tea seed (Camelia sinensis) oils, *J. King Saud Univ., Sci.*, 2013, **25**, 149–155.

20 Z. Sun, C. Lian, C. Li and S. Zheng, Investigations on organo-montmorillonites modified by binary nonionic/zwitterionic surfactant mixtures for simultaneous adsorption of aflatoxin B1 and zearalenone, *J. Colloid Interface Sci.*, 2020, **565**, 11–22.

21 Y. Tan, C. Li, Z. Sun, C. Liang and S. Zheng, Ternary structural assembly of $BiOCl/TiO_2$/clinoptilolite composite: study of coupled mechanism and photocatalytic performance, *J. Colloid Interface Sci.*, 2020, **564**, 143–154.

22 S. Yang, Z. Huang, P. Wu, Y. Li, X. Dong, C. Li, N. Zhu, X. Duan and D. D. Dionysiou, Rapid removal of tetrabromobisphenol A by α-Fe_2O_3-*x*@ Graphene@ Montmorillonite catalyst with oxygen vacancies through peroxymonosulfate activation: role of halogen and α-hydroxyalkyl radicals, *Appl. Catal., B*, 2020, **260**, 118129.

23 X. Dong, B. Ren, Z. Sun, C. Li, X. Zhang, M. Kong, S. Zheng and D. D. Dionysiou, Monodispersed $CuFe_2O_4$ nanoparticles anchored on natural kaolinite as highly efficient peroxymonosulfate catalyst for bisphenol A degradation, *Appl. Catal., B*, 2019, **253**, 206–217.

24 Q. Gu, T. C. A. Ng, Y. Bao, H. Y. Ng, S. C. Tan and J. Wang, Developing better ceramic membranes for water and wastewater Treatment: Where microstructure integrates with chemistry and functionalities, *Chem. Eng. J.*, 2022, **428**, 130456.

25 D. Zou and Y. Fan, State-of-the-art developments in fabricating ceramic membranes with low energy consumption, *Ceram. Int.*, 2021, **47**, 14966–14987.

26 S. K. Hubadillah, M. R. Jamalludin, M. H. D. Othman and Y. Iwamoto, Recent progress on low-cost ceramic membrane for water and wastewater treatment, *Ceram. Int.*, 2022, 24157–24191.

27 A. Heidari, A. Shahbazi, T. M. Aminabhavi, D. Barceló and S. Rtimi, A systematic review of clay-based photocatalysts for emergent micropollutants removal and microbial inactivation from aqueous media: status and limitations, *J. Environ. Chem. Eng.*, 2022, 108813.

28 S. K. Hubadillah, M. H. D. Othman, T. Matsuura, A. Ismail, M. A. Rahman, Z. Harun, J. Jaafar and M. Nomura, Fabrications and applications of low cost ceramic membrane from kaolin: A comprehensive review, *Ceram. Int.*, 2018, **44**, 4538–4560.

29 W. Zhu, Y. Liu, K. Guan, C. Peng and J. Wu, Design and optimization of ceramic membrane structure: from the perspective of flux matching between support and membrane, *Ceram. Int.*, 2021, **47**, 12357–12365.

30 N. Ahmed and F. Q. Mir, Fabrication of a cost effective ceramic microfiltration membrane by utilizing local Kashmir clay, *Trans. Indian Ceram. Soc.*, 2021, **80**, 41–46.

31 J. Anandkumar, B. P. Sahariah and S. Dasgupta, Synthesize and characterization of clay based low-cost membrane for solid-liquid separation, *Recent Res. Sci. Technol.*, 2014, **6**, 14–17.

32 B. Das, B. Chakrabarty and P. Barkakati, Preparation and characterization of novel ceramic membranes for microfiltration applications, *Ceram. Int.*, 2016, **42**, 14326–14333.

33 F. Azaman, M. Nor, W. R. W. Abdullah, M. H. Razali, R. C. Zulkifli, M. A. A. Zaini and A. Ali, Review on natural clay ceramic membrane: Fabrication and application in water and wastewater treatment, *Malays. J. Fundam. Appl. Sci.*, 2021, **17**, 62–78.

34 T. Mohammadi and A. Pak, Effect of calcination temperature of kaolin as a support for zeolite membranes, *Sep. Purif. Technol.*, 2003, **30**, 241–249.

35 M. Bengisu and M. Bengisu, *Engineering Ceramics*, Springer, 2001.

36 S. Bousbih, E. Errais, F. Darragi, J. Duplay, M. Trabelsi-Ayadi, M. O. Daramola and R. Ben Amar, Treatment of textile wastewater using monolayered ultrafiltation ceramic membrane fabricated from natural kaolin clay, *Environ. Technol.*, 2021, **42**, 3348–3359.

37 S. K. Hubadillah, Universiti Tun Hussein Onn Malaysia, 2015.

38 D. Vasanth, R. Uppaluri and G. Pugazhenthi, Influence of sintering temperature on the properties of porous ceramic support prepared by uniaxial dry compaction method using low-cost raw materials for membrane applications, *Sep. Sci. Technol.*, 2011, **46**, 1241–1249.

39 K. Suresh and G. Pugazhenthi, Cross flow microfiltration of oil-water emulsions using clay based ceramic membrane support and TiO_2 composite membrane, *Egypt. J. Pet.*, 2017, **26**, 679–694.

40 S. Loeb and S. Sourirajan, *Sea water demineralization by means of an osmotic membrane*, ACS Publications, 1962.

41 J. Luyten, A. Buekenhoudt, W. Adriansens, J. Cooymans, H. Weyten, F. Servaes and R. Leysen, Preparation of $LaSrCoFeO_{3-x}$ membranes, *Solid State Ionics*, 2000, **135**, 637–642.

42 B. F. Kingsbury and K. Li, A morphological study of ceramic hollow fibre membranes, *J. Membr. Sci.*, 2009, **328**, 134–140.

43 M. H. D. Othman, N. Droushiotis, Z. Wu, G. Kelsall and K. Li, Dual-layer hollow fibres with different anode structures for micro-tubular solid oxide fuel cells, *J. Power Sources*, 2012, **205**, 272–280.

44 M. H. Abd Aziz, M. H. D. Othman, N. A. Hashim, M. R. Adam and A. Mustafa, Fabrication and characterization of mullite ceramic hollow fiber membrane from natural occurring ball clay, *Appl. Clay Sci.*, 2019, **177**, 51–62.

45 T. Ahmad, C. Guria and A. Mandal, Optimal synthesis and operation of low-cost polyvinyl chloride/bentonite ultrafiltration membranes for the purification of oilfield produced water, *J. Membr. Sci.*, 2018, **564**, 859–877.

46 C. G. Ugwuja, O. O. Adelowo, A. Ogunlaja, M. O. Omorogie, O. D. Olukanni, O. O. Ikhimiukor, I. Iermak, G. A. Kolawole, C. Guenter and A. Taubert, Visible-light-

mediated photodynamic water disinfection@ bimetallic-doped hybrid clay nanocomposites, *ACS Appl. Mater. Interfaces*, 2019, **11**, 25483–25494.

47 M. O. Alfred, M. O. Omorogie, O. Bodede, R. Moodley, A. Ogunlaja, O. G. Adeyemi, C. Günter, A. Taubert, I. Iermak and H. Eckert, Solar-active clay-TiO_2 nanocomposites prepared via biomass assisted synthesis: Efficient removal of ampicillin, sulfamethoxazole and artemether from water, *Chem. Eng. J.*, 2020, **398**, 125544.

48 S. P. Patil, V. Shrivastava, G. Sonawane and S. Sonawane, Synthesis of novel Bi_2O_3–montmorillonite nanocomposite with enhanced photocatalytic performance in dye degradation, *J. Environ. Chem. Eng.*, 2015, **3**, 2597–2603.

49 H. Peng, D. Wu, H. Wan, L. Jia, G. Chen, J. Li, Y. Cao, X. Liu and R. Ma, Facile synthesis and characterization of halloysite@ $W_{18}O_{49}$ nanocomposite with enhanced photocatalytic properties, *Appl. Clay Sci.*, 2019, **183**, 105319.

50 H. S. Zakria, M. H. D. Othman, R. Kamaludin, S. H. S. A. Kadir, T. A. Kurniawan and A. Jilani, Immobilization techniques of a photocatalyst into and onto a polymer membrane for photocatalytic activity, *RSC Adv.*, 2021, **11**, 6985–7014.

51 S. Riaz and S.-J. Park, An overview of TiO_2-based photocatalytic membrane reactors for water and wastewater treatments, *J. Ind. Eng. Chem.*, 2020, **84**, 23–41.

52 L. Djafer, A. Ayral and A. Ouagued, Robust synthesis and performance of a titania-based ultrafiltration membrane with photocatalytic properties, *Sep. Purif. Technol.*, 2010, **75**, 198–203.

53 H.-J. Hong, S. K. Sarkar and B.-T. Lee, Formation of TiO_2 nano fibers on a micro-channeled Al_2O_3–ZrO_2/TiO_2 porous composite membrane for photocatalytic filtration, *J. Eur. Ceram. Soc.*, 2012, **32**, 657–663.

54 S. Obregón and V. Rodríguez-González, Photocatalytic TiO_2 thin films and coatings prepared by sol–gel processing: A brief review, *J. Sol-Gel Sci. Technol.*, 2021, 1–17.

55 N. Neethu and T. Choudhury, Treatment of methylene blue and methyl orange dyes in wastewater by grafted titania pillared clay membranes, *Recent Pat. Nanotechnol.*, 2018, **12**, 200–207.

56 A. Bouazizi, M. Breida, B. Achiou, M. Ouammou, J. I. Calvo, A. Aaddane and S. A. Younssi, Removal of dyes by a new nano–TiO_2 ultrafiltration membrane deposited on low-cost support prepared from natural Moroccan bentonite, *Appl. Clay Sci.*, 2017, **149**, 127–135.

57 S. Khemakhem and R. B. Amar, Grafting of fluoroalkylsilanes on microfiltration Tunisian clay membrane, *Ceram. Int.*, 2011, **37**, 3323–3328.

58 H. Shi, G. Chen, C. Zhang and Z. Zou, Polymeric g-C_3N_4 coupled with $NaNbO_3$ nanowires toward enhanced photocatalytic reduction of CO_2 into renewable fuel, *ACS Catal.*, 2014, **4**, 3637–3643.

59 M. Yan, G. Li, C. Guo, W. Guo, D. Ding, S. Zhang and S. Liu, WO_{3-x} sensitized TiO_2 spheres with full-spectrum-driven photocatalytic activities from UV to near infrared, *Nanoscale*, 2016, **8**, 17828–17835.

60 Y. A. Shaban and M. I. Orif, Purification of seawater by C–Cu–TiO_2 ceramic based membrane, *Desalin. Water Treat.*, 2019, **162**, 60–69.

61 X. Chen, Y. Hu, Z. Xie and H. Wang, in *Current Trends and Future Developments on (Bio-) Membranes*, Elsevier, 2018, pp. 71–96.

62 P. Burmann, B. Zornoza, C. Téllez and J. Coronas, Mixed matrix membranes comprising MOFs and porous silicate fillers prepared via spin coating for gas separation, *Chem. Eng. Sci.*, 2014, **107**, 66–75.

63 A. Bouazizi, M. Breida, A. Karim, B. Achiou, M. Ouammou, J. Calvo, A. Aaddane, K. Khiat and S. A. Younssi, Development of a new TiO_2 ultrafiltration membrane on flat ceramic support made from natural bentonite and micronized phosphate and applied for dye removal, *Ceram. Int.*, 2017, **43**, 1479–1487.

64 M. Mouiya, A. Bouazizi, A. Abourriche, A. Benhammou, Y. El Hafiane, M. Ouammou, Y. Abouliatim, S. A. Younssi, A. Smith and H. Hannache, Fabrication and characterization of a ceramic membrane from clay and banana peel powder: Application to industrial wastewater treatment, *Mater. Chem. Phys.*, 2019, **227**, 291–301.

65 S. Saja, A. Bouazizi, B. Achiou, H. Ouaddari, A. Karim, M. Ouammou, A. Aaddane, J. Bennazha and S. A. Younssi, Fabrication of low-cost ceramic ultrafiltration membrane made from bentonite clay and its application for soluble dyes removal, *J. Eur. Ceram. Soc.*, 2020, **40**, 2453–2462.

66 B. J. Deka, J. Guo, N. K. Khanzada and A. K. An, Omniphobic re-entrant PVDF membrane with ZnO nanoparticles composite for desalination of low surface tension oily seawater, *Water Res.*, 2019, **165**, 114982.

67 M. H. Abd Aziz, M. A. B. Pauzan, N. A. S. M. Hisam, M. H. D. Othman, M. R. Adam, Y. Iwamoto, M. H. Puteh, M. A. Rahman, J. Jaafar and A. F. Ismail, Superhydrophobic ball clay based ceramic hollow fibre membrane via universal spray coating method for membrane distillation, *Sep. Purif. Technol.*, 2022, **288**, 120574.

68 E. Alebrahim, F. Tarasi, M. S. Rahaman, A. Dolatabadi and C. Moreau, Fabrication of titanium dioxide filtration membrane using suspension plasma spray process, *Surf. Coat. Technol.*, 2019, **378**, 124927.

69 X. Liu, K. Wen, C. Deng, K. Yang, C. Deng, M. Liu and K. Zhou, Nanostructured photocatalytic TiO_2 coating deposited by suspension plasma spraying with different injection positions, *J. Therm. Spray Technol.*, 2018, **27**, 245–254.

70 E. Alebrahim, M. S. Rahaman and C. Moreau, TiO_2 photocatalytic ultrafiltration membrane developed with suspension plasma spray process, *Coatings*, 2022, **12**, 1764.

71 D. Liang, J. Huang, H. Zhang, H. Fu, Y. Zhang and H. Chen, Influencing factors on the performance of tubular ceramic membrane supports prepared by extrusion, *Ceram. Int.*, 2021, **47**, 10464–10477.

72 D. Vasanth, G. Pugazhenthi and R. Uppaluri, Fabrication and properties of low cost ceramic microfiltration membranes for separation of oil and bacteria from its solution, *J. Membr. Sci.*, 2011, **379**, 154–163.

73 N. H. Mohtor, M. H. D. Othman, A. F. Ismail, M. A. Rahman, J. Jaafar and N. A. Hashim, Investigation on the effect of sintering temperature on kaolin hollow fibre membrane for dye filtration, *Environ. Sci. Pollut. Res.*, 2017, **24**, 15905–15917.
74 Z. Liu, Q. Cheng, Y. Wang, Y. Li and J. Zhang, Sintering neck growth mechanism of Fe nanoparticles: A molecular dynamics simulation, *Chem. Eng. Sci.*, 2020, **218**, 115583.
75 A. Harabi, F. Zenikheri, B. Boudaira, F. Bouzerara, A. Guechi and L. Foughali, A new and economic approach to fabricate resistant porous membrane supports using kaolin and $CaCO_3$, *J. Eur. Ceram. Soc.*, 2014, **34**, 1329–1340.
76 M. R. Adam, M. H. D. Othman, M. H. Puteh, A. Ismail, A. Mustafa, M. A. Rahman and J. Jaafar, Impact of sintering temperature and pH of feed solution on adsorptive removal of ammonia from wastewater using clinoptilolite based hollow fibre ceramic membrane, *J. Water Process Eng.*, 2020, **33**, 101063.
77 N. Malik, V. K. Bulasara and S. Basu, Preparation of novel porous ceramic microfiltration membranes from fly ash, kaolin and dolomite mixtures, *Ceram. Int.*, 2020, **46**, 6889–6898.
78 Z. Wei, J. Hou and Z. Zhu, High-aluminum fly ash recycling for fabrication of cost-effective ceramic membrane supports, *J. Alloys Compd.*, 2016, **683**, 474–480.
79 S. Jana, M. Purkait and K. Mohanty, Preparation and characterizations of ceramic microfiltration membrane: effect of inorganic precursors on membrane morphology, *Sep. Sci. Technol.*, 2010, **46**, 33–45.
80 M. Mohamed Bazin, N. Ahmad and Y. Nakamura, Preparation of porous ceramic membranes from Sayong ball clay, *J. Asian Ceram. Soc.*, 2019, **7**, 417–425.
81 M. Mouiya, A. Bouazizi, A. Abourriche, Y. El Khessaimi, A. Benhammou, Y. Taha, M. Oumam, Y. Abouliatim, A. Smith and H. Hannache, Effect of sintering temperature on the microstructure and mechanical behavior of porous ceramics made from clay and banana peel powder, *Results Mater.*, 2019, **4**, 100028.
82 M. N. Rahaman, *Ceramic processing and sintering*, CRC press, 2017.
83 M. Rawat and V. K. Bulasara, Synthesis and characterization of low-cost ceramic membranes from fly ash and kaolin for humic acid separation, *Korean J. Chem. Eng.*, 2018, **35**, 725–733.
84 S. B. Rekik, J. Bouaziz, A. Deratani and S. Beklouti, Study of ceramic membrane from naturally occurring-kaolin clays for microfiltration applications, *Period. Polytech., Chem. Eng.*, 2017, **61**, 206–215.
85 B. Boudaira, A. Harabi, F. Bouzerara, F. Zenikheri, L. Foughali and A. Guechi, Preparation and characterization of membrane supports for microfiltration and ultrafiltration using kaolin (DD2) and $CaCO_3$, *Desalin. Water Treat.*, 2016, **57**, 5258–5265.
86 Z. Zhu, Z. Wei, W. Sun, J. Hou, B. He and Y. Dong, Cost-effective utilization of mineral-based raw materials for preparation of porous mullite ceramic membranes via *in situ* reaction method, *Appl. Clay Sci.*, 2016, **120**, 135–141.
87 S. K. Hubadillah, Z. Harun, M. H. D. Othman, A. Ismail, W. N. W. Salleh, H. Basri, M. Z. Yunos and P. Gani, Preparation and characterization of low cost porous ceramic membrane support from kaolin using phase inversion/sintering technique for gas separation: Effect of kaolin content and non-solvent coagulant bath, *Chem. Eng. Res. Des.*, 2016, **112**, 24–35.
88 M. Lee, Z. Wu, R. Wang and K. Li, Micro-structured alumina hollow fibre membranes–Potential applications in wastewater treatment, *J. Membr. Sci.*, 2014, **461**, 39–48.
89 R. Meghnani, M. Kumar, G. Pugazhenthi and V. Dhakshinamoorthy, Synthesis of ceramic membrane using inexpensive precursors and evaluation of its biocompatibility for hemofiltration application, *Sep. Purif. Technol.*, 2021, **256**, 117814.
90 A. Dhivya and A. Keshav, Fabrication of ball clay based low-cost ceramic membrane supports and their characterization for microfiltration application, *J. Indian Chem. Soc.*, 2022, **99**, 100557.
91 A. Agarwalla and K. Mohanty, Comprehensive characterization, development, and application of natural/Assam Kaolin-based ceramic microfiltration membrane, *Mater. Today Chem.*, 2022, **23**, 100649.
92 C. M. Kumar, M. Roshni and D. Vasanth, Treatment of aqueous bacterial solution using ceramic membrane prepared from cheaper clays: A detailed investigation of fouling and cleaning, *J. Water Process Eng.*, 2019, **29**, 100797.
93 J.-H. Eom, Y.-W. Kim, S.-H. Yun and I.-H. Song, Low-cost clay-based membranes for oily wastewater treatment, *J. Ceram. Soc. Jpn.*, 2014, **122**, 788–794.
94 A. Buekenhoudt, A. Kovalevsky, J. Luyten and F. Snijkers, 1.11—Basic Aspects in Inorganic Membrane Preparation, *Comprehensive Membrane Science and Engineering*, ed. E. Drioli and L. Giorno, 2010, pp. 217–252.
95 S. P. David and D. Sarkar, Porous Ceramics, *Ceramic Processing: Industrial Practices*, 2019, p. 101.
96 S. Chakraborty, R. Uppaluri and C. Das, Effect of pore former (saw dust) characteristics on the properties of submicron range low-cost ceramic membranes, *Int. J. Ceram. Eng. Sci.*, 2020, **2**, 243–253.
97 D. Li, Y. Qu, J. Liu, W. He, H. Wang and Y. Feng, Using ammonium bicarbonate as pore former in activated carbon catalyst layer to enhance performance of air cathode microbial fuel cell, *J. Power Sources*, 2014, **272**, 909–914.
98 L. Mingyi, Y. Bo, X. Jingming and C. Jing, Influence of pore formers on physical properties and microstructures of supporting cathodes of solid oxide electrolysis cells, *Int. J. Hydrogen Energy*, 2010, **35**, 2670–2674.
99 L. A. Xavier, T. V. de Oliveira, W. Klitzke, A. B. Mariano, D. Eiras and R. B. Vieira, Influence of thermally modified clays and inexpensive pore-generating and strength improving agents on the properties of porous ceramic membrane, *Appl. Clay Sci.*, 2019, **168**, 260–268.
100 M. M. Lorente-Ayza, E. Sánchez, V. Sanz and S. Mestre, Influence of starch content on the properties of low-cost

microfiltration ceramic membranes, *Ceram. Int.*, 2015, **41**, 13064–13073.

101 Q. F. Bao, W. X. Dong, J. E. Zhou, Y. Q. Wang and Y. Liu, Effects of pore former on properties of alumina porous ceramic for application in micro-filtration membrane supports, *Key Eng. Mater.*, 2015, **655**, 97–102.

102 P. Kudryavtsev, Main routes of the porous composite materials creation, *Nanotechnol. Constr. Sci. Int.*, 2020, **12**, 256–269.

103 K. J. Falua, A. Pokharel, A. Babaei-Ghazvini, Y. Ai and B. Acharya, Valorization of starch to biobased materials: A review, *Polymers*, 2022, **14**, 2215.

104 K. Mohanta, A. Kumar, O. Parkash and D. Kumar, Processing and properties of low cost macroporous alumina ceramics with tailored porosity and pore size fabricated using rice husk and sucrose, *J. Eur. Ceram. Soc.*, 2014, **34**, 2401–2412.

105 N. Ahmed and F. Q. Mir, Preparation and characterization of ceramic membrane using waste almond shells as pore forming agent, *Mater. Today: Proc.*, 2021, **47**, 1485–1489.

106 Q. Lü, X. Dong, Z. Zhu and Y. Dong, Environment-oriented low-cost porous mullite ceramic membrane supports fabricated from coal gangue and bauxite, *J. Hazard. Mater.*, 2014, **273**, 136–145.

107 D. O. Obada, D. Dodoo-Arhin, M. Dauda, F. O. Anafi, A. S. Ahmed and O. A. Ajayi, Physico-mechanical and gas permeability characteristics of kaolin based ceramic membranes prepared with a new pore-forming agent, *Appl. Clay Sci.*, 2017, **150**, 175–183.

108 A. R. Jamaludin, S. R. Kasim, M. Z. Abdullah and Z. A. Ahmad, Sago starch as binder and pore-forming agent for the fabrication of porcelain foam, *Ceram. Int.*, 2014, **40**, 4777–4784.

109 L. Ferrage, G. Bertrand, P. Lenormand, D. Grossin and B. Ben-Nissan, A review of the additive manufacturing (3DP) of bioceramics: Alumina, zirconia (PSZ) and hydroxyapatite, *J. Aust. Ceram. Soc.*, 2017, **53**, 11–20.

110 J.-H. Ha, S. Z. A. Bukhari, J. Lee, I.-H. Song and C. Park, Preparation processes and characterizations of alumina-coated alumina support layers and alumina-coated natural material-based support layers for microfiltration, *Ceram. Int.*, 2016, **42**, 13796–13804.

111 H. Chen, X. Li, J. Wei, Y. Feng and D. Gao, Preparation and properties of coal ash ceramic membranes for water and heat recovery from flue gas, *J. Chem.*, 2019, **2019**, 1–10.

112 S. K. Amin, M. H. Roushdy, H. A. Abdallah, A. F. Moustafa and M. F. Abadir, Preparation and characterization of ceramic nanofiltration membrane prepared from hazardous industrial waste, *Int. J. Appl. Ceram. Technol.*, 2020, **17**, 162–174.

113 H. R. Mahdavi, M. Arzani and T. Mohammadi, Synthesis, characterization and performance evaluation of an optimized ceramic membrane with physical separation and photocatalytic degradation capabilities, *Ceram. Int.*, 2018, **44**, 10281–10292.

114 P. Singh, N. A. Manikandan, M. Purnima, K. Pakshirajan and G. Pugazhenthi, Recovery of lignin from water and methanol using low-cost kaolin based tubular ceramic membrane, *J. Water Process Eng.*, 2020, **38**, 101615.

115 M. Boussemghoune, M. Chikhi, Y. Ozay, P. Guler, B. Ozbey Unal and N. Dizge, The investigation of organic binder effect on morphological structure of ceramic membrane support, *Symmetry*, 2020, **12**, 770.

116 S. Bose and C. Das, Role of binder and preparation pressure in tubular ceramic membrane processing: design and optimization study using response surface methodology (RSM), *Ind. Eng. Chem. Res.*, 2014, **53**, 12319–12329.

117 N. Ahmed and F. Q. Mir, Box–Behnken design for optimization of iron removal by hybrid oxidation–microfiltration process using ceramic membrane, *J. Mater. Sci.*, 2022, **57**, 15224–15238.

118 S. Correia, D. Hotza and A. Segadães, Simultaneous optimization of linear firing shrinkage and water absorption of triaxial ceramic bodies using experiments design, *Ceram. Int.*, 2004, **30**, 917–922.

119 A. Khalfaoui, M. Hajjaji, S. Kacim and A. Baçaoui, Evaluation of the simultaneous effects of firing cycle parameters on technological properties and ceramic suitability of a raw clay using the response surface methodology, *J. Am. Ceram. Soc.*, 2006, **89**, 1563–1567.

120 M. A. Baih, H. Saffaj, K. Aziz, A. Bakka, H. Zidouh, R. Mamouni and N. Saffaj, Statistical optimization of the elaboration of ceramic membrane support using Plackett-Burman and response surface methodology, *Mater. Today: Proc.*, 2022, **52**, 128–136.

121 B. Sarde and Y. Patil, Recent research status on polymer composite used in concrete-an overview, *Mater. Today: Proc.*, 2019, **18**, 3780–3790.

122 M. Arzani, H. R. Mahdavi, O. Bakhtiari and T. Mohammadi, Preparation of mullite ceramic microfilter membranes using Response surface methodology based on central composite design, *Ceram. Int.*, 2016, **42**, 8155–8164.

123 B. Varol and N. Uzal, Arsenic removal from aqueous solutions by ultrafiltration assisted with polyacrylamide: an application of response surface methodology, *Desalin. Water Treat.*, 2015, **56**, 736–743.

124 R. H. Myers, D. C. Montgomery, G. G. Vining, C. M. Borror and S. M. Kowalski, Response surface methodology: a retrospective and literature survey, *J. Qual. Technol.*, 2004, **36**, 53–77.

125 D. Montgomery, Discovering dispersion effects, *Design and Analysis of Experiments*, John Wiley, New york, Section, 5th edn, 2001, vol. 3.

126 N. Elhadiri, M. Benchanaa, R. Chikri, R. Idouhli and K. Tabit, Low-cost and high-performance ceramic membrane from sugar industry waste: characterization and optimization using experimental design, *Mater. Today: Proc.*, 2022, **53**, 310–317.

127 D. Njoya, M. Hajjaji and D. Njopwouo, Effects of some processing factors on technical properties of a clay-based ceramic material, *Appl. Clay Sci.*, 2012, **65**, 106–113.

128 P. Kumari, N. Bahadur and L. F. Dumée, Photo-catalytic membrane reactors for the remediation of persistent

organic pollutants–A review, *Sep. Purif. Technol.*, 2020, **230**, 115878.

129 S. Mitra, A. J. Chakraborty, A. M. Tareq, T. B. Emran, F. Nainu, A. Khusro, A. M. Idris, M. U. Khandaker, H. Osman and F. A. Alhumaydhi, Impact of heavy metals on the environment and human health: Novel therapeutic insights to counter the toxicity, *J. King Saud Univ., Sci.*, 2022, **34**, 101865.

130 S. Ye, Y. Chen, X. Yao and J. Zhang, Simultaneous removal of organic pollutants and heavy metals in wastewater by photoelectrocatalysis: A review, *Chemosphere*, 2021, **273**, 128503.

131 M. N. Subramaniam, P. S. Goh, D. Kanakaraju, J. W. Lim, W. J. Lau and A. F. Ismail, Photocatalytic membranes: a new perspective for persistent organic pollutants removal, *Environ. Sci. Pollut. Res.*, 2022, **29**, 12506–12530.

132 M. Baniamer, A. Aroujalian and S. Sharifnia, Photocatalytic membrane reactor for simultaneous separation and photoreduction of CO_2 to methanol, *Int. J. Energy Res.*, 2021, **45**, 2353–2366.

133 H. Zheng, X. Meng, Y. Yang, J. Chen and S. Huo, Bifunctional photocatalytic nanofiltration membranes with immobilized $BaTiO_3/Ti_3C_2T_x$ catalysts for the simultaneous separation and degradation of azo compounds, *J. Environ. Chem. Eng.*, 2023, **11**, 110064.

134 K. Staszak, Membrane processes, *Phys. Sci. Rev.*, 2017, **2**, 20170142.

135 X. Shen, T. Zhang, P. Xu, L. Zhang, J. Liu and Z. Chen, Growth of C_3N_4 nanosheets on carbon-fiber cloth as flexible and macroscale filter-membrane-shaped photocatalyst for degrading the flowing wastewater, *Appl. Catal., B*, 2017, **219**, 425–431.

136 S. Abd Hamid, M. Shahadat, B. Ballinger, S. F. Azha, S. Ismail, S. W. Ali and S. Z. Ahammad, Role of clay-based membrane for removal of copper from aqueous solution, *J. Saudi Chem. Soc.*, 2020, **24**, 785–798.

137 T. Choudhury, Clay Hybrid Membranes in Wastewater Treatment, *Clay Clay Miner.*, 2021, 197.

138 B. Szczepanik, Photocatalytic degradation of organic contaminants over clay-TiO_2 nanocomposites: A review, *Appl. Clay Sci.*, 2017, **141**, 227–239.

139 H. Chang, H. Liang, F. Qu, B. Liu, H. Yu, X. Du, G. Li and S. A. Snyder, Hydraulic backwashing for low-pressure membranes in drinking water treatment: A review, *J. Membr. Sci.*, 2017, **540**, 362–380.

140 É. N. Santos, Z. László, C. Hodúr, G. Arthanareeswaran and G. Veréb, Photocatalytic membrane filtration and its advantages over conventional approaches in the treatment of oily wastewater: a review, *Methods*, 2020, **13**, 14.

141 D. Chen, Q. Zhu, F. Zhou, X. Deng and F. Li, Synthesis and photocatalytic performances of the TiO_2 pillared montmorillonite, *J. Hazard. Mater.*, 2012, **235**, 186–193.

142 S. Rameshkumar, R. Henderson and R. B. Padamati, Improved surface functional and photocatalytic properties of hybrid ZnO-MoS_2-deposited membrane for photocatalysis-assisted dye filtration, *Membranes*, 2020, **10**, 106.

143 S. Lin, S. Sun, K. Shen, D. Tan, H. Zhang, F. Dong and X. Fu, Photocatalytic microreactors based on nano TiO_2-containing clay colloidosomes, *Appl. Clay Sci.*, 2018, **159**, 42–49.

144 J. Domenzain-Gonzalez, J. J. Castro-Arellano, L. A. Galicia-Luna, M. Rodriguez-Cruz, R. T. Hernandez-Lopez and L. Lartundo-Rojas, Photocatalytic membrane reactor based on Mexican Natural Zeolite: RB5 dye removal by photo-Fenton process, *J. Environ. Chem. Eng.*, 2021, **9**, 105281.